



Chapter 5

Protracted Magmatic-Hydrothermal History of the Río Blanco-Los Bronces District, Central Chile: Development of World's Greatest Known Concentration of Copper

JUAN CARLOS TORO,¹ JAVIER ORTÚZAR,^{2,†} JORGE ZAMORANO,¹ PATRICIO CUADRA,³ JUAN HERMOSILLA,³ AND CRISTIAN SPRÖHNLE⁴

¹Anglo American Chile, Gerencia de Exploraciones, Av. Pedro de Valdivia 291, Providencia, Santiago, Chile

²Anglo American Exploration (Australia), Suite 1, 16 Brodie-Hall Drive, Bentley, 6102, Western Australia, Australia

³Codelco-Chile, División Andina, Sta. Teresa 513, Los Andes, Chile

⁴Compañía Minera Doña Inés de Collahuasi, Av. Baquedano 902, Iquique, Chile

Abstract

The Río Blanco-Los Bronces copper-molybdenum porphyry district in the late Miocene to early Pliocene magmatic arc of central Chile is currently being mined by state mining company CODELCO (Río Blanco) and Anglo American Sur (Los Bronces). Combined annual production in 2011 was nearly 450,000 metric tons (t) of copper plus by-product molybdenum. With Anglo American's recent high-grade discoveries in the district (3.7 billion tons (Bt) grading 0.7% Cu at San Enrique-Monolito, and 4.5 Bt grading 0.9% Cu at Los Sulfatos) adding more than 65 Mt of fine copper to the mineral inventory, the district now ranks as the world's largest by contained metal, with more than 200 Mt of copper.

Volcanic and volcaniclastic rocks of the Abanico and Farellones Formations represent premineralization host rocks ranging in age between 22.7 ± 0.4 and 16.8 ± 0.3 Ma (U-Pb dating of zircons). The bulk of the copper-molybdenum porphyry endowment is related to evolution of the San Francisco batholith, a large (200 km^2) granodiorite-dominated complex with U-Pb zircon ages between 16.4 ± 0.2 to 8.4 ± 0.2 Ma.

Three geologic domains are defined in the district on the basis of rock types, structural breaks, and age determinations: the Los Piches-Ortiga block in the west, the San Manuel-El Plomo block in the center, and the Río Blanco-Los Bronces-Los Sulfatos block in the east. These geologic domains are younger progressively to the east, with most of the known copper endowment on the easternmost (Río Blanco-Los Bronces-Los Sulfatos) block. Intrusive and hydrothermal activity in the Los Piches-Ortiga block spanned ~2.5 m.y., from 14.8 ± 0.1 to 12.3 ± 0.1 Ma. Although these events apparently did not produce high-grade copper deposits, silver-bearing veins associated with a high sulfidation hydrothermal system are present in the block. To the east, in the San Manuel-El Plomo block, a series of magmatic-hydrothermal systems developed during a ~3-m.y. period between 10.8 ± 0.1 and 7.7 ± 0.1 Ma. These events also apparently failed to generate high-grade copper systems. Magmatic-hydrothermal activity in the eastern Río Blanco-Los Bronces-Los Sulfatos block, hosting virtually all of the copper endowment recognized in the district, spanned a ~4-m.y. period from 8.2 ± 0.5 to 4.31 ± 0.05 Ma.

Copper endowment in the district is associated with vertically continuous breccia bodies and quartz-vein-stockworked porphyries. Hydrothermal assemblages follow a characteristic vertical and lateral zonation pattern. Remnants of high sulfidation and/or advanced argillic assemblages (quartz-enargite-tennantite-galena-sphalerite-gypsum-anhydrite with dumortierite-pyrophyllite-alunite) and peripheral sericite-illite reflect preservation of shallow levels, whereas K-silicate alteration assemblages (biotite-K-feldspar-albite) are present in association with chalcopyrite-bornite and chalcopyrite-pyrite at depth. Between the mineralized bodies, a distal assemblage of hydrothermal chlorite-epidote-specularite-pyrite predominates. At Río Blanco-Los Bronces, igneous and/or hydrothermal- and hydrothermal-cemented breccias developed in intimate association with porphyry phases. At shallow depths, the hydrothermal breccia cement generally comprises quartz-sericite-tourmaline, and contains pyrite > chalcopyrite/molybdenite. At deeper levels the breccia cement is predominantly biotite-K-feldspar containing bornite-chalcopyrite-molybdenite. These progressively grade outward into chalcopyrite-pyrite-dominated zones and ultimately to pyrite-dominated zones. Within the Río Blanco-Los Bronces-Los Sulfatos block, the upper presence of the K-silicate assemblage varies from ~3,000 m above sea level (a.s.l.) in the poorly telescoped northern area (Río Blanco), to ~4,000 m a.s.l in the highly telescoped southern area (Los Sulfatos). These differences may reflect varying rates of synmineral structural exhumation, or varying depth of porphyry emplacement along the Río Blanco-Los Bronces-Los Sulfatos structural corridor.

Key factors contributing to the copper productivity in the district are considered to reflect both far-field tectonic conditions, and district-scale structural controls. Following the last significant phase of volcanism documented in the district (~16.8 Ma), a temporally discrete period of peak compression and rapid exhumation, between ~6 to 3 Ma, affected the central Chilean Andes. This period of uplift relates to flat-slab subduction of sea floor containing the Juan Fernandez Ridge into the Chile Trench and overlaps part of the emplacement history of the Río Blanco-Los Bronces-Los Sulfatos block (8.2–4.31 Ma). The lack of contemporaneous

[†]Corresponding author: e-mail, javier.ortuzar@angloamerican.com

volcanism and concomitant tectonic uplift are interpreted to reflect a state of increased horizontal crustal compression due to shear coupling of the downgoing slab. By suppressing volcanism, these conditions are considered to promote the retention of magma in the deep crustal environment, where higher pressures promote greater solubility of magmatic volatiles and higher temperatures may promote longer lived magma chambers by slowing fractionation processes. Under such conditions, the potential is enhanced for increased amounts of metals and volatiles by addition of fresh batches of magma to the deep magma chamber. At the district scale, closely spaced (2 km) structures that control the position of the porphyry and breccia bodies in the Río Blanco-Los Bronces-Los Sulfatos block appear to have focused long-lived, multistage magmatic-hydrothermal activity within a narrow structural corridor, contributing to the development of large, high-grade porphyry/breccia systems.

Introduction

THE RÍO BLANCO-Los Bronces copper-molybdenum porphyry district is located in the late Miocene to early Pliocene magmatic arc of central Chile, approximately 50 km northeast of Santiago at elevations between 3,000 and 4,800 m above sea level (a.s.l.; Fig. 1). Here in the high cordillera, at elevations between 3,000 and 4,800 meters above sea level (m a.s.l.), copper and molybdenum are currently being mined by two companies: Anglo American Sur, which operates the Los

Bronces open-pit mine, and Corporación Nacional del Cobre de Chile (CODELCO), which operates the Río Blanco block-cave mine and the Sur Sur open pit. In 2011, Los Bronces and Río Blanco produced 221,800 and 234,000 metric tons (t) of copper, respectively, with historic production from all operations in the district estimated to be 9.5 million metric tons (Mt) of copper (Camus, 2003; Anglo American, unpub. data). While Camus (2003) estimated the potential remaining copper resource of the district to be approximately 57 Mt of copper, subsequent exploration discoveries at both Los Bronces and Río Blanco, as well as elsewhere in the district, have since elevated this resource figure substantially. With a global resource exceeding 200 Mt of copper (Table 1), the Río Blanco-Los Bronces district is currently the world's most endowed porphyry copper cluster.

This paper presents a current overview of the Río Blanco-Los Bronces district. It is a joint effort of geologists of Anglo American and CODELCO combining geologic and (largely unpublished) geochronological datasets to provide an update of the geology and magmatic-hydrothermal evolution of the Río Blanco-Los Bronces district.

History and Development of the Río Blanco-Los Bronces District

Figure 2 provides a timeline summarizing the long and complex exploration and development history of the Río

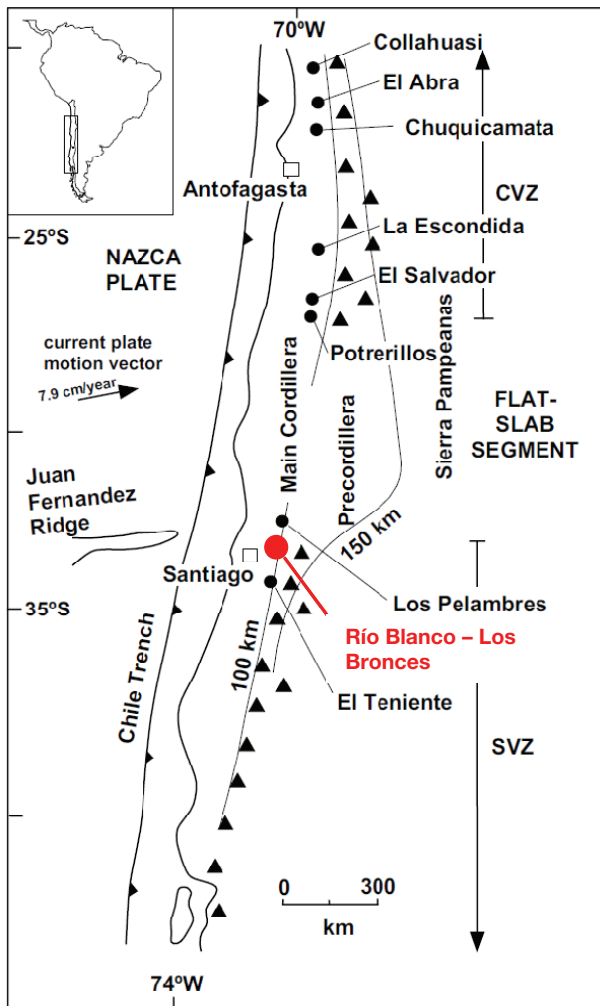


FIG. 1. Map of the central Chilean Andes, showing major porphyry copper deposits in relationship to the flat-slab section of the Chilean subduction zone and the location of the Juan Fernandez Ridge. Modified after Serrano et al. (1996). Triangles = active volcanoes, circles = ore deposits, CVZ = Central Volcanic Zone, SVZ = Southern Volcanic Zone.

TABLE 1. Mineral Inventory Estimates, Río Blanco-Los Bronces District (modified from Irarrazaval et al., 2010)

Area	Resources (Mt)	Cu (%)	Contained Cu (Mt)
Andina			
Deposit resources ¹	16,908	0.63	106.5
Los Bronces			
Los Bronces reserve (flotation) ²	1,498	0.62	9.3
Los Bronces reserve (dump leach) ²	684	0.33	2.3
Los Bronces resource (flotation) ²	3,199	0.39	12.5
Los Bronces resource (dump leach) ²	114	0.26	0.3
San Enrique-Monolito deposit ³	3,700	0.7	25.9
Los Sulfatos deposits (target-size resources) ⁴	4,500	0.9	40.5
Subtotal			197.2
Historic production ⁵			9.5
Total contained copper			206.7

Data sources:

¹ Olavarria (2009)

² Anglo American plc (2012)

³ Anglo American plc (2009a)

⁴ Anglo American plc (2009b)

⁵ Camus (2003)

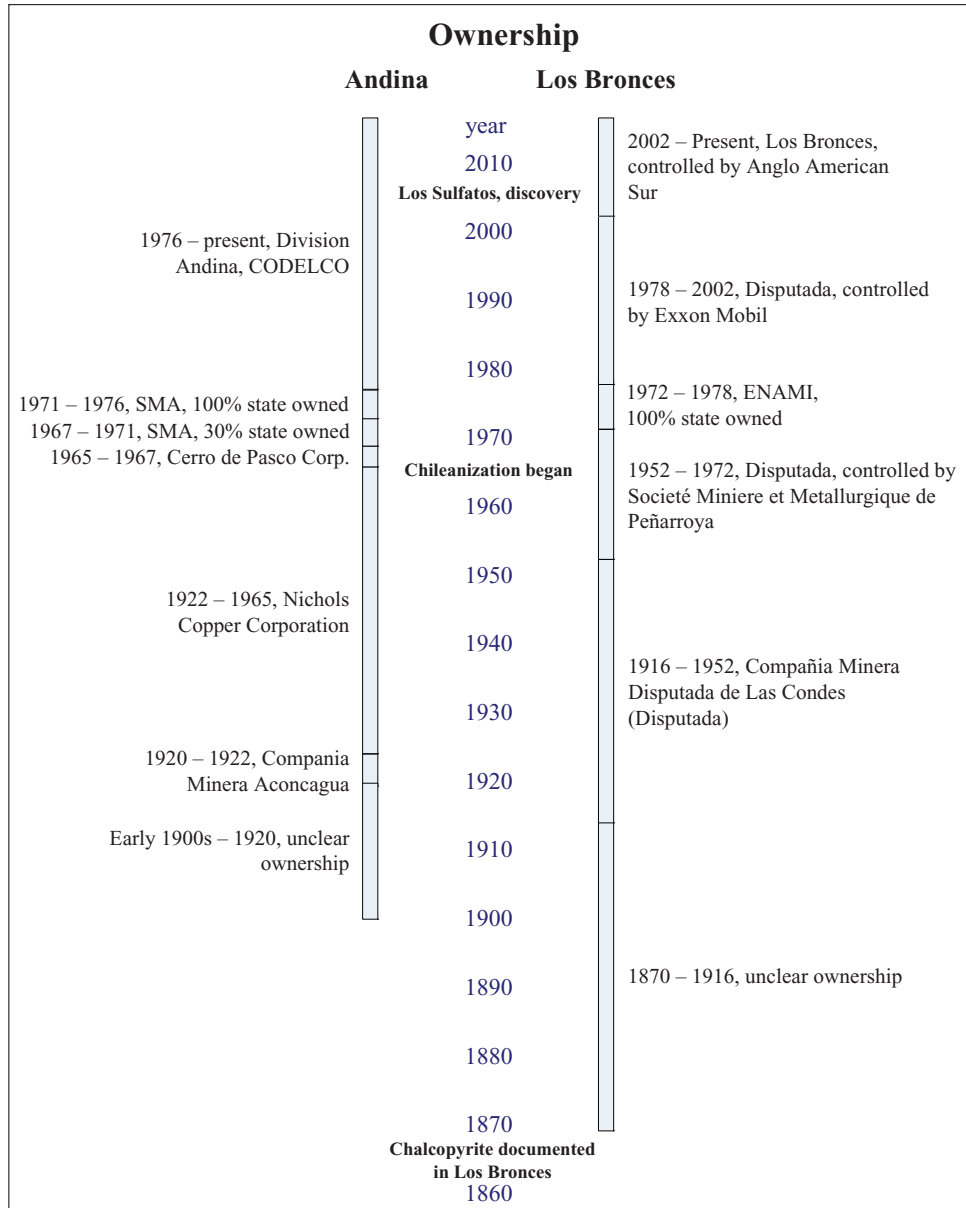


FIG. 2. Summary of the mineral tenement ownership of the Rio Blanco-Los Bronces district.

Blanco-Los Bronces district. The history for Los Bronces in particular is adapted from Irarrazaval et al. (2010).

In 1864 workers from the nearby Las Condes farm observed partially snow-covered outcrops of massive, bronce (the informal miner's name for chalcopyrite) in the headwaters of the San Francisco River (Warnaars et al., 1985; Baeza, 1990). Small-scale mining followed in the 1870s and 1880s, with manual exploitation of high-grade (25% Cu) ore. By the early 1900s, up to ten vertical shafts with depths of >100 m continued to exploit massive to semimassive chalcopyrite (>23% Cu) during the Austral summer seasons. At this time, the complex ownership of the mining district (ten different producing companies; R.H. Sales, unpub. report for Andes Exploration Company, 1916) led to operational inefficiencies and boundary disputes. When Los Bronces was eventually

consolidated in 1916, the frequent legal disputes over mining rights that had plagued it since discovery resulted in the new company being aptly named Compañía Minera Disputada de Las Condes (Disputed mining company of Las Condes). At the beginning of the 20th century, there were a number of mines in production at Los Bronces, among them Disputada, which sent its high-grade ore to the Perez Caldera smelter, but there were only minor mine workings at Río Blanco.

In 1920, the engineer Felix Corona established the first mining company (Compañía Minera Aconcagua) at the Río Blanco deposit. In 1922, Corona sold the property to North American Nichols Copper Corporation, which consolidated the district mining property rights in 1965 as Compañía Minera Andina, a wholly owned subsidiary of the Cerro de Pasco Corporation.

In 1952, the French company Société Minière et Métallurgique de Peñarroya acquired Disputada (W. Swayne, unpub. report for Anaconda Copper Mining Company, 1958). During this period, the process of government involvement in the Chilean copper mining industry ("chileanization") was advancing, with the creation of the Corporación del Cobre in 1966. In 1967, Law 16.624 was issued by the Chilean government and the "chileanization" process began. As a consequence, the Sociedad Minera Andina was created from the assets of the Compañía Minera Andina, in which the Chilean state controlled 30% and Cerro de Pasco the balance (Correa, 1975). The subsequent democratic election of the socialist government of Salvador Allende heralded the nationalization of the entire Chilean copper mining industry. In 1972, during the Allende government, almost 99% of Compañía Minera Disputada de Las Condes (also including the El Soldado mine and the Los Chagres smelter) was purchased by the state mining agency Empresa Nacional de Minería (ENAMI) for US\$5M.

Up until the 1973 coup d'état led by General Augusto Pinochet, the nationalized Chilean mines were kept under state control. In 1976, the military government established CODELCO to operate Chile's large copper mines and the División Andina was created from Sociedad Minera Andina and became one of the operational divisions of CODELCO. Following six years of operation, Disputada was considered a noncore asset by the Chilean government, and the company was privatized once again via an international tender, eventually being purchased in 1978 by an affiliate of Exxon Mobil Corporation for US\$97 million (Warnaars et al., 1985). Based on the positive results of an extensive drilling program, Exxon initiated a major expansion in 1989, and this was commissioned in 1993.

In mid-2001, Anglo American conducted due diligence studies of Disputada after Exxon Mobile determined that Disputada was a noncore asset. Anglo American's geologic review team concluded that not only did the existing Los Bronces orebody have the potential for resources to support substantial future expansions, but also that the La Paloma sector had characteristics consistent with potential for 350 to 500 Mt of additional mineralized material at grades between 0.5 to 1.0% copper. The review team speculated that Los Sulfatos was a contiguous extension of the overall La Paloma-Los Sulfatos system, implying significant further upside potential (V. Irarrazaval and J.C. Toro, unpub. report for Empresa Minera de Mantos Blancos S.A., 2001).

In November 2002, Exxon Mobil sold Disputada to Anglo American for US\$1.300M. Anglo American completed a major expansion of Los Bronces in 2011, investing US\$2.200M. Concurrently, the brownfield exploration team discovered two additional major centers of mineralization, La Paloma-Los Sulfatos (now referred to as the Los Sulfatos deposit) and San Enrique-Monolito, which together have added 65 Mt of contained copper to the mineral resource base of the district (Irarrazaval, 2010; Table 1).

Geologic Setting

The late Miocene to early Pliocene porphyry copper belt that hosts Río Blanco-Los Bronces lies near the southern end of a Neogene metallogenic belt that extends for ~6,000 km along the Andes from west-central Colombia to central Chile

and west-central Argentina (Fig. 1). From late Eocene to early Miocene (~36–20 Ma), continental tholeiitic to calc-alkaline volcanism (Los Pelambres, Abanico, and Coya Machalí Formations) accumulated in a N-S-elongated, extensional intra-arc basin. Between latitudes 31° and 35° S, the Miocene-Pliocene magmatic evolution of the southern portion of the belt in central Chile and west-central Argentina may be assigned to two main stages (Sillitoe and Perelló, 2005; Perelló et al., 2009, and references therein): (1) early to late Miocene (~18 to <15, possibly 6 Ma), tholeiitic to calc-alkaline basaltic, dacitic, and rhyolitic volcanic rocks erupted from stratovolcanoes and dome complexes (Farellones Formation) and granodiorite plutons and porphyry copper-bearing stocks emplaced between ~12 and 8 Ma; and (2) late Miocene to early Pliocene (~8.19–4.5 Ma) porphyry formation at Río Blanco-Los Bronces and El Teniente, followed by postmineralization emplacement of lamprophyre dikes (4–3 Ma) at El Teniente (Maksaev et al., 2004; Deckart et al., 2005). The Río Blanco-Los Bronces and El Teniente porphyry deposits occupy the transition between a domain of low-angle "flat-slab" subduction section of the Nazca oceanic plate (between 28°–33° S) and a domain with a subduction dip angle of 25°–30° to the south. The flat-slab segment corresponds to a conspicuous "volcanic gap" lacking in significant modern volcanic activity, while the segment to the south coincides with the current active Southern Volcanic Zone of the Andes (Stern, 1989; Cahill and Isaaks, 1992; Skewes and Stern, 1995; Fig. 1). The flattening of the subduction zone is related to the southward progression of subduction of the Juan Fernández Ridge under the South American continental plate (Fig. 1). Passage of this flexure in the downgoing slab appears to coincide with the major mineralizing events at Los Bronces-Río Blanco and El Teniente (Stern, 1989; Skewes and Holmgren, 1993; Skewes and Stern, 1995; Kurtz et al., 1997; Kay and Mpodozis, 2002; Ramos et al., 2002; Hollings et al., 2005).

Copper-molybdenum introduction at the main deposits and/or clusters along the Miocene-Pliocene belt, namely Los Pelambres-El Pachón, Río Blanco-Los Bronces, and El Teniente, occurred in relationship to multiphase stocks and dikes of quartz-monzonite, quartz monzodiorite, granodiorite, and quartz diorite porphyry (Fig. 1). These highly oxidized, medium to high K calc-alkaline phases intruded the Cenozoic igneous rocks, including a mafic sill complex at El Teniente (Skewes et al., 2002). Copper-bearing hydrothermal-cemented breccias are a significant ore component at Río Blanco-Los Bronces, and El Teniente, and are present in smaller volumes at Los Pelambres-El Pachón (e.g., Serrano et al., 1996; Vargas et al., 1999; Camus, 2003; Cannell et al., 2005; Perelló et al., 2009). Late- to postmineralization diatreme breccias at Río Blanco-Los Bronces and especially at El Teniente appear to have disrupted appreciable volumes of preexisting mineralized rocks.

District Geology

This summary of the geology and geochronology of the Río Blanco-Los Bronces district reflects the recent work of Anglo American Exploration and CODELCO and builds upon published studies of specific deposits (e.g., Serrano et al., 1996; Vargas et al., 1999; Deckart et al., 2005; Frikken et al., 2005;

and references therein) to develop a district-wide synthesis. This study presents 77 U-Pb, Re-Os and $^{40}\text{Ar}/^{39}\text{Ar}$ age determinations (Tables 2, 3), considered to represent the timing of igneous crystallization and hydrothermal activity in the district. Deckart et al. (2005) concluded that several previously published Ar-Ar and K-Ar age determinations for the district represented thermal resetting of the K-Ar isotope system by repeated and widespread postmineralization intrusive activity in the Río Blanco-Los Bronces district.

Subhorizontal to gently folded volcanic and volcanioclastic rocks of the Abanico and Farellones Formations underlie much of the Río Blanco-Los Bronces district (Fig. 3). The bulk of the copper-molybdenum porphyry endowment is related to evolution of the San Francisco batholith, a granodiorite-dominated complex with an exposed extent of at least 200 km² that intruded the Abanico and Farellones Formations (Fig. 3). The premineralization volcanic rocks of the Farellones Formation yielded U-Pb zircon ages between 22.7 ± 0.4 and 16.8 ± 0.3 Ma and the San Francisco batholith range from 16.4 ± 0.2 to 8.4 ± 0.2 Ma (Table 3; Fig. 4).

On the basis of rock types, structural breaks, and age determinations, three geologic domains are defined in the district. These include the Los Piches-Ortiga block in the west, the San Manuel-El Plomo block in the center, and the Río Blanco-Los Bronces-Los Sulfatos block in the east (Fig. 5).

Los Piches-Ortiga block (14.8–12.3 Ma)

The Los Piches-Ortiga block contains the earliest evidence of hydrothermal activity identified to date in the district. The block has a N-S trend and measures 8 × 2 km at surface (Figs. 3, 5). In the southwestern part of the block, strong and widespread Na-Ca-Fe (actinolite-tremolite-scapolite-chlorite-epidote-apatite-biotite and local pyrite-chalcopyrite) metasomatism affected the volcanic and intrusive rocks. The metasomatism also affected contemporaneous late-magmatic breccias (Table 4). Farther west, strong potassic metasomatism with weak early biotite veinlets and A-type veinlets (Gustafson and Hunt, 1975; Gustafson and Quiroga, 1995; Table 5) occurs within quartz-monzonite facies of the San Francisco batholith. Hydrothermal quartz-tourmaline-sericite-pyrite-cemented breccias cut the quartz-monzonite stock. A structural graben is present west of the Ortiga area, where a siliceous lithocap of advanced argillic alteration (quartz, pyrophyllite, alunite, kaolinite, and pyrite) is preserved (Figs. 3, 5).

TABLE 2. Summary of Geochronological Methods Used in This Study

Samples by geochronological method	Samples by mineral/type of vein
16 $^{238}\text{U}-^{206}\text{Pb}$ CA-TIMS	15 Re/Os, molybdenite, B-type veins, early stage
9 $^{238}\text{U}-^{206}\text{Pb}$ ID-TIMS	4 Re/Os, molybdenite, late stage
6 $^{238}\text{U}-^{206}\text{Pb}$ SHRIMP	9 $^{40}\text{Ar}/^{39}\text{Ar}$, secondary biotite
10 $^{238}\text{U}-^{206}\text{Pb}$ LA-ICPMS	7 $^{40}\text{Ar}/^{39}\text{Ar}$, sericite
17 $^{40}\text{Ar}/^{39}\text{Ar}$	1 $^{40}\text{Ar}/^{39}\text{Ar}$, hypogene alunite
19 Re-Os	41 $^{238}\text{U}-^{206}\text{Pb}$, zircon

Notes: CA-TIMS = chemical abrasion-thermal ionization mass spectrometry, ID-TIMS = isotope dilution-thermal ionization mass spectrometry, SHRIMP = sensitive high-resolution ion microprobe, LA-ICPMS = laser ablation-inductively coupled plasma mass spectrometry

Veins associated with quartz-barite-alunite-kaolinite-specularite-siderite, and containing enargite-tennantite-tetrahedrite/freibergite-bornite-chalcopyrite, are present 3 km east of Los Piches Prospect (Fig. 3). These veins were exploited for silver between 1920 and 1940 (S. Barassi, C. Castro, and C. Walker, unpub. report for Compania Minera Disputada de Las Condes, 2004; J.C. Toro, unpub. report for Anglo American Chile Ltda., 2012).

San Manuel-El Plomo block (10.8–7.7 Ma)

East of the Los Piches-Ortiga block, NW-trending structures extending for up to 6 km define a corridor ~3 km in width containing the San Manuel-El Plomo block (Figs. 3, 5). Here contact metamorphism (hornfelsing) has affected the wall rocks, where quartz-monzonite porphyries of the San Francisco batholith have intruded volcanic and volcanioclastic rocks of the Abanico and Farellones Formations.

Two hydrothermal centers are identified: San Manuel and El Plomo (Figs. 3, 5a, b; geologic sections Z-Z' and A-A'). Alteration assemblages containing hydrothermal biotite (at El Plomo), and biotite-K-feldspar with disseminated chalcopyrite-bornite at San Manuel affect the andesites and have overprinted the aforementioned assemblages. N-NW-oriented tourmaline-sericite-cemented breccias (10–70 m long × 2–15 m wide), containing disseminated chalcopyrite-pyrite cut the porphyry intrusions and the volcanic and volcanioclastic rocks at San Manuel and El Plomo (Table 4). An assemblage of chlorite-magnetite-epidote-calcite overprints the late-magmatic breccias (Table 4) at El Plomo and San Manuel. An assemblage of kaolinite-illite-sericite-montmorillonite with disseminated chalcopyrite and pyrite affects all the aforementioned units. Limited exploration to date suggests low to moderate copper and molybdenum grades in both areas (0.1–0.5% Cu; C. Sprohnle, unpub. report for Anglo American Chile Ltda, 2007).

At El Plomo, U-Pb ages determined for the earliest recognized porphyry phases (quartz monzodiorite porphyry) from 10.8 ± 0.1 to 10.77 ± 0.1 Ma (Table 3; Fig. 4) are slightly older than the $^{40}\text{Ar}/^{39}\text{Ar}$ ages obtained for sericite from the tourmaline-cemented breccia (10.6 ± 0.2 Ma) and for secondary biotite from the andesite (10.1 ± 0.1 Ma; Table 3; Fig. 4). At San Manuel, a U-Pb age determined for feldspar porphyry (10.2 ± 0.3 Ma) is considerably older than an Re-Os molybdenite age determined for the earliest recognized hydrothermal event (8.36 ± 0.06) and a $^{40}\text{Ar}/^{39}\text{Ar}$ age obtained for secondary biotite from a fine quartz-monzonite porphyry (7.7 ± 0.1 Ma; Table 3; Fig. 4).

Río Blanco-Los Bronces-Los Sulfatos block (8.2–4.3 Ma)

The Río Blanco-Los Bronces-Los Sulfatos block comprises the district's principal magmatic-hydrothermal systems and contains nearly all the currently economic mineralization recognized therein (Figs. 3, 5). N-NW-trending structures, extending for up to 10 km, define a mineralized corridor ~2 km in width. Emplacement of dike swarms, breccias, and associated mineralization within the block appears to have followed deep-seated N-NW-trending basement faults defining the Río Blanco-Los Bronces structural corridor (Silva et al., 2009; Figs. 3, 5). Foliation developed within plagioclase phenocrysts and hydrothermal biotite, subparallel quartz veins,

TABLE 3. Summary of Geochronologic Data from the Río Blanco-Los Bronces District

Geological unit	Site	Lithology/vein type/mineral	Mineral	Method	Age ($\pm 2\sigma$)	Longitude	Latitude	Elevation (m) ¹	Reference ²
Farellones Formation	Potrero Alto	Dacite tuff	Zircon	$^{206}\text{Pb}/^{238}\text{U}$ SHRIMP	22.7 ± 0.4	-	-	-	1
Farellones Formation	La Americana	Andesite	Zircon	$^{206}\text{Pb}/^{238}\text{U}$ SHRIMP	17.2 ± 0.1	-	-	-	2
Farellones Formation	Rio Blanco	Andesite	Zircon	$^{206}\text{Pb}/^{238}\text{U}$ ID-TIMS	17.20 ± 0.05	-	-	-	3
Farellones Formation	Don Luis	Andesite	Zircon	$^{206}\text{Pb}/^{238}\text{U}$ ID-TIMS	16.8 ± 0.3	-	-	-	3
San Francisco Complex	La Copa	Biotite sienogranite	Zircon	$^{206}\text{Pb}/^{238}\text{U}$ SHRIMP	16.4 ± 0.2	-	-	-	1
San Francisco Complex	Yerba Loca	Quartz monzonite	Zircon	$^{206}\text{Pb}/^{238}\text{U}$ CA-TIMS	15.0 ± 0.2	-	-	-	4
San Francisco Complex	Yerba Loca	Quartz monzonite	Zircon	$^{206}\text{Pb}/^{238}\text{U}$ CA-TIMS	14.9 ± 0.2	-	-	-	4
Ortiga-Los Piches	Los Piches	Quartz monzonite	Biotite	$^{40}\text{Ar}/^{39}\text{Ar}$	14.8 ± 0.1	-	-	-	5
San Francisco Complex	8 km south of Los Bronces mine	Quartz monzonite	Zircon	$^{206}\text{Pb}/^{238}\text{U}$ LA-ICPMS	14.7 ± 0.1	-	-	-	4
Ortiga-Los Piches	Los Piches	Tourmaline-cemented breccia	Sericite	$^{40}\text{Ar}/^{39}\text{Ar}$	13.7 ± 0.3	$70^\circ 20' 3.48''$	$33^\circ 12' 3.48''$	2741	6
Ortiga-Los Piches	Los Piches	Feldspar porphyry	Zircon	$^{206}\text{Pb}/^{238}\text{U}$ LA-ICPMS	13.4 ± 0.1	$70^\circ 20' 14.59''$	$33^\circ 12' 14.59''$	2792	6
Ortiga-Los Piches	Los Piches	Tourmaline-cemented breccia	Sericite	$^{40}\text{Ar}/^{39}\text{Ar}$	12.8 ± 0.3	$70^\circ 20' 14.59''$	$33^\circ 12' 14.59''$	2792	6
Ortiga-Los Piches	Ortiga	Andesite (lithocap)	Hypogene alunite	$^{40}\text{Ar}/^{39}\text{Ar}$	12.3 ± 0.1	$70^\circ 22' 21.97''$	$33^\circ 9' 21.97''$	3284	7
San Francisco Complex	Rio Blanco	Granodiorite	Zircon	$^{206}\text{Pb}/^{238}\text{U}$ ID-TIMS	12.0 ± 0.4	-	-	-	3
San Francisco Complex	Los Bronces mine	Granodiorite	Zircon	$^{206}\text{Pb}/^{238}\text{U}$ LA-ICPMS	11.2 ± 0.1	-	-	-	4
El Plomo	El Plomo	Quartz monzodiorite	Zircon	$^{206}\text{Pb}/^{238}\text{U}$ LA-ICPMS	10.8 ± 0.1	$70^\circ 18' 19.38''$	$33^\circ 6' 19.38''$	3748	4
El Plomo	El Plomo	Quartz monzodiorite	Zircon	$^{206}\text{Pb}/^{238}\text{U}$ LA-ICPMS	10.77 ± 0.1	$70^\circ 18' 17.58''$	$33^\circ 6' 17.58''$	3864	6
El Plomo	El Plomo	Tourmaline-cemented breccia	Sericite	$^{40}\text{Ar}/^{39}\text{Ar}$	10.6 ± 0.2	$70^\circ 18' 18.49''$	$33^\circ 6' 18.49''$	3872	6
San Manuel	San Manuel	Feldspar porphyry	Zircon	$^{206}\text{Pb}/^{238}\text{U}$ LA-ICPMS	10.2 ± 0.3	$70^\circ 17' 30.92''$	$33^\circ 8' 30.92''$	3738	6
El Plomo	El Plomo	Andesite	Biotite	$^{40}\text{Ar}/^{39}\text{Ar}$	10.1 ± 0.1	$70^\circ 22' 0.74''$	$36^\circ 4' 0.74''$	3600	6
San Francisco Complex	Don Luis	Diorite	Zircon	$^{206}\text{Pb}/^{238}\text{U}$ ID-TIMS	8.84 ± 0.05	-	-	-	3
San Francisco Complex	Don Luis	Diorite	Zircon	$^{206}\text{Pb}/^{238}\text{U}$ CA-TIMS	8.8 ± 0.2	-	-	-	8
San Francisco Complex	Rio Blanco	Diorite porphyry	Zircon	$^{206}\text{Pb}/^{238}\text{U}$ LA-ICPMS	8.5 ± 0.1	$70^\circ 15' 53.44''$	$33^\circ 8' 53.44''$	2596	6
San Francisco Complex	Rio Blanco	Cascada granodiorite	Zircon	$^{206}\text{Pb}/^{238}\text{U}$ ID-TIMS	8.4 ± 0.2	-	-	-	3
San Manuel	San Manuel	Tourmaline-cemented breccia	Molybdenite	Re/Os	8.36 ± 0.06	$70^\circ 17' 16.39''$	$33^\circ 8' 16.39''$	3765	6
Rio Blanco	Don Luis	Diorite	Zircon	$^{206}\text{Pb}/^{238}\text{U}$ LA-ICPMS	8.2 ± 0.5	-	-	-	3
San Manuel	San Manuel	Fine quartz monzonite	Biotite	$^{40}\text{Ar}/^{39}\text{Ar}$	7.7 ± 0.1	$70^\circ 17' 24.58''$	$33^\circ 8' 24.58''$	2545	6
Condell	Condell	Diorite porphyry	Biotite	$^{40}\text{Ar}/^{39}\text{Ar}$	7.61 ± 0.08	$70^\circ 9' 59.22''$	$33^\circ 4' 59.22''$	4192	9
Los Sulfatos	Los Sulfatos	Tourmaline-cemented breccia, B-type vein	Molybdenite	Re/Os	7.45 ± 0.05	-	-	-	9
Los Sulfatos	Los Sulfatos	Tourmaline-cemented breccia, B-type vein	Molybdenite	Re/Os	7.42 ± 0.05	-	-	-	9
Los Sulfatos	Los Sulfatos	Biotite-cemented breccia	Biotite	$^{40}\text{Ar}/^{39}\text{Ar}$	7.3 ± 0.1	$70^\circ 14' 15.67''$	$33^\circ 12' 15.67''$	3969	9
San Enrique Monolito	San Enrique-Monolito	Quartz monzonite, EB-type vein	Biotite	$^{40}\text{Ar}/^{39}\text{Ar}$	7.2 ± 0.2	-	-	-	6
Los Sulfatos	Los Sulfatos	Los Sulfatos porphyry, secondary biotite	Biotite	$^{40}\text{Ar}/^{39}\text{Ar}$	7.14 ± 0.08	$70^\circ 14' 22.39''$	$33^\circ 12' 22.39''$	4163	9
Rio Blanco	Rio Blanco	Quartz monzonite	Zircon	$^{206}\text{Pb}/^{238}\text{U}$ CA-TIMS	7.1 ± 0.2	$70^\circ 15' 24.81''$	$33^\circ 8' 4.81''$	2387	8
Los Sulfatos	Los Sulfatos	Los Sulfatos porphyry, secondary biotite	Biotite	$^{40}\text{Ar}/^{39}\text{Ar}$	7.00 ± 0.1	$70^\circ 14' 20.27''$	$33^\circ 12' 0.27''$	4347	9
Los Sulfatos	Los Sulfatos	Los Sulfatos porphyry, D-type vein	Sericite	$^{40}\text{Ar}/^{39}\text{Ar}$	6.94 ± 0.06	$70^\circ 14' 17.84''$	$33^\circ 12' 17.84''$	4293	9
Rio Blanco	Rio Blanco	Quartz monzonite	Zircon	$^{206}\text{Pb}/^{238}\text{U}$ CA-TIMS	6.8 ± 0.3	-	-	-	10
Los Sulfatos	Los Sulfatos	Granodiorite porphyry	Sericite	$^{40}\text{Ar}/^{39}\text{Ar}$	6.71 ± 0.04	$70^\circ 14' 6.27''$	$33^\circ 12' 6.27''$	4062	9
Rio Blanco	Rio Blanco	Granodiorite, EBT-type vein	Molybdenite	Re/Os	6.70 ± 0.03	$70^\circ 15' 0.26''$	$33^\circ 8' 0.26''$	2937	10
Los Sulfatos	Los Sulfatos	Los Sulfatos porphyry, B-type vein	Molybdenite	Re/Os	6.56 ± 0.05	-	-	-	9
La Americana	La Americana	Dacite porphyry	Zircon	$^{206}\text{Pb}/^{238}\text{U}$ SHRIMP	6.5 ± 0.1	-	-	-	2

TABLE 3. (Cont.)

Geological unit	Site	Lithology/vein type/mineral	Mineral	Method	Age ($\pm 2\sigma$)	Longitude	Latitude	Elevation (m) ¹	Reference ²
Rio Blanco	Rio Blanco	Quartz monzonite porphyry	Zircon	$^{206}\text{Pb}/^{238}\text{U}$ CA-TIMS	6.51 ± 0.03	$70^\circ 15' 16.31''$	$33^\circ 8' 6.31''$	2639	4
Rio Blanco	Rio Blanco	Quartz monzonite porphyry	Zircon	$^{206}\text{Pb}/^{238}\text{U}$ CA-TIMS	6.48 ± 0.05	$70^\circ 15' 38.75''$	$33^\circ 8' 38.75''$	2921	4
Rio Blanco	Rio Blanco	Granodiorite, EBT-type vein	Molybdenite	Re/Os	6.48 ± 0.03	-	-	-	4
Rio Blanco	Rio Blanco	Quartz monzonite porphyry	Zircon	$^{206}\text{Pb}/^{238}\text{U}$ SHRIMP	6.32 ± 0.09	-	-	-	3
Los Sulfatos	Los Sulfatos	La Paloma porphyry, B-type vein	Molybdenite	Re/Os	6.26 ± 0.05	-	-	-	9
Rio Blanco	Rio Blanco	Rock-flour breccia, B vein	Molybdenite	Re/Os	6.07 ± 0.03	$70^\circ 15' 29.52''$	$33^\circ 8' 29.52''$	3070	4
San Enrique Monolito	San Enrique-Monolito	Observatorio porphyry	Zircon	$^{206}\text{Pb}/^{238}\text{U}$ LA-ICPMS	6.0 ± 0.1	$70^\circ 15' 42.49''$	$33^\circ 9' 42.49''$	3503	6
La Americana	La Americana	Dacite porphyry	Zircon	$^{206}\text{Pb}/^{238}\text{U}$ CA-TIMS	6.0 ± 0.1	-	-	-	2
Don Luis	Don Luis	Diorite, B-type vein	Molybdenite	Re/Os	5.96 ± 0.03	$70^\circ 15' 53.31''$	$33^\circ 8' 53.31''$	2947	4
Rio Blanco	Rio Blanco	Feldspar porphyry	Zircon	$^{206}\text{Pb}/^{238}\text{U}$ CA-TIMS	5.92 ± 0.03	$70^\circ 15' 20.90''$	$33^\circ 8' 20.90''$	2980	4
Rio Blanco	Rio Blanco	Quartz monzonite porphyry	Zircon	$^{206}\text{Pb}/^{238}\text{U}$ CA-TIMS	5.84 ± 0.06	$70^\circ 15' 20.14''$	$33^\circ 8' 20.14''$	3004	4
Don Luis	Don Luis	Feldspar porphyry	Zircon	$^{206}\text{Pb}/^{238}\text{U}$ ID-TIMS	5.84 ± 0.03	-	-	-	3
Sur Sur	Sur Sur	Tourmaline-cemented breccia, B-type vein	Molybdenite	Re/Os	5.79 ± 0.03	$70^\circ 15' 21.40''$	$33^\circ 8' 21.40''$	3055	8
Rio Blanco	Rio Blanco	Tourmaline-cemented breccia, B-type vein	Molybdenite	Re/Os	5.79 ± 0.03	$70^\circ 15' 38.69''$	$33^\circ 9' 8.69''$	3270	4
Rio Blanco	Rio Blanco	Feldspar porphyry	Zircon	$^{206}\text{Pb}/^{238}\text{U}$ CA-TIMS	5.7 ± 0.1	$70^\circ 15' 36.40''$	$33^\circ 9' 36.40''$	2947	8
Rio Blanco	Mina	Fine quartz monzonite, B-type vein	Molybdenite	Re/Os	5.65 ± 0.03	$70^\circ 15' 43.27''$	$33^\circ 9' 43.27''$	3226	6
Sur Sur	Sur Sur	Tourmaline-cemented breccia, B-type vein	Molybdenite	Re/Os	5.52 ± 0.03	$70^\circ 15' 34.09''$	$33^\circ 9' 34.09''$	3163	4
Don Luis	Don Luis	Feldspar porphyry	Zircon	$^{206}\text{Pb}/^{238}\text{U}$ CA-TIMS	5.47 ± 0.01	$70^\circ 15' 46.09''$	$33^\circ 8' 46.09''$	3071	4
Sur Sur	Sur Sur	Tourmaline-cemented breccia	Sericite	$^{40}\text{Ar}/^{39}\text{Ar}$	5.42 ± 0.09	-	-	-	11
Don Luis	Don Luis	Don Luís porphyry	Zircon	$^{206}\text{Pb}/^{238}\text{U}$ CA-TIMS	5.35 ± 0.04	$70^\circ 15' 57.52''$	$33^\circ 8' 57.52''$	3260	4
Los Bronces	Los Bronces	Fine quartz monzonite, B-type vein	Molybdenite	Re/Os	5.35 ± 0.03	$70^\circ 15' 43.39''$	$33^\circ 9' 43.39''$	3164	6
Rio Blanco	Rio Blanco	Breccia complex	Molybdenite	Re/Os	5.31 ± 0.03	-	-	-	12
Rio Blanco	Rio Blanco	Breccia complex	Molybdenite	Re/Os	5.25 ± 0.05	-	-	-	12
Don Luis	Don Luis	Don Luís porphyry	Zircon	$^{206}\text{Pb}/^{238}\text{U}$ ID-TIMS	5.23 ± 0.07	-	-	-	3
Don Luis	Don Luis	Don Luís porphyry	Zircon	$^{206}\text{Pb}/^{238}\text{U}$ CA-TIMS	5.16 ± 0.04	-	-	-	4
Don Luis	Don Luis	Don Luís porphyry	Zircon	$^{206}\text{Pb}/^{238}\text{U}$ CA-TIMS	5.0 ± 0.1	$70^\circ 15' 46.09''$	$33^\circ 8' 46.09''$	3071	4
La Copo	La Copo	Dacite plug, subvolcanic complex	Zircon	$^{206}\text{Pb}/^{238}\text{U}$ LA-ICPMS	4.92 ± 0.09	-	-	-	3
Don Luis	Don Luis	Don Luis porphyry, B-type vein	Molybdenite	Re/Os	4.9 ± 0.02	$70^\circ 15' 48.08''$	$33^\circ 8' 48.08''$	3500	4
Don Luis	Don Luis	Don Luis porphyry, B-type vein	Molybdenite	Re/Os	4.89 ± 0.02	$70^\circ 15' 57.68''$	$33^\circ 8' 7.68''$	2778	8
Don Luis	Don Luis	Don Luis porphyry, B-type vein	Molybdenite	Re/Os	4.87 ± 0.02	$70^\circ 15' 46.15''$	$33^\circ 8' 46.15''$	3070	4
Sur Sur	Sur Sur	Biotite-cemented breccia	Biotite	$^{40}\text{Ar}/^{39}\text{Ar}$	4.78 ± 0.04	-	-	-	11
La Copo	La Copo	Dacite chimmyey	Zircon	$^{206}\text{Pb}/^{238}\text{U}$ ID-TIMS	4.78 ± 0.08	$70^\circ 15' 30.40''$	$33^\circ 8' 30.40''$	2821	4
La Copo	La Copo	Dacite chimmyey with sericitic alteration	Sericite	$^{40}\text{Ar}/^{39}\text{Ar}$	4.71 ± 0.08	$70^\circ 15' 32.20''$	$33^\circ 8' 32.20''$	3009	4
La Copo	La Copo	Dacite chimmyey	Zircon	$^{206}\text{Pb}/^{238}\text{U}$ ID-TIMS	4.57 ± 0.08	-	-	-	4
La Copo	La Copo	Andesitic dike	Zircon	$^{206}\text{Pb}/^{238}\text{U}$ CA-TIMS	4.57 ± 0.04	$70^\circ 15' 6.32''$	$33^\circ 8' 6.32''$	2810	4
La Copo	La Copo	Rhyolite chimmyey	Zircon	$^{206}\text{Pb}/^{238}\text{U}$ SHRIMP	4.31 ± 0.05	$70^\circ 15' 11.04''$	$33^\circ 8' 11.04''$	3500	4

¹ Elevation relative to sea level² References: 1 = J. Piquer, unpub. report for CODELCO, 2010; 2 = A. Bertens and E. Wettke, unpub. report for CODELCO, 2009; 3 = Deckart et al., 2005; 4 = A. Bertens et al., unpub. report for CODELCO, 2010; 5 = Serrano et al., 1996; 6 = Deckart et al., 2009; 7 = Eggers, 2009; 8 = Deckart et al., 2012; 9 = J.C. Toro and J. Ortúzar, unpub. report for Anglo American Chile, Ltda., 2008; 10 = A. Bertens and J. Hermosilla, unpub. report for CODELCO, 2010; 11 = Frikken et al., 2005; 12 = Mathur et al., 2001

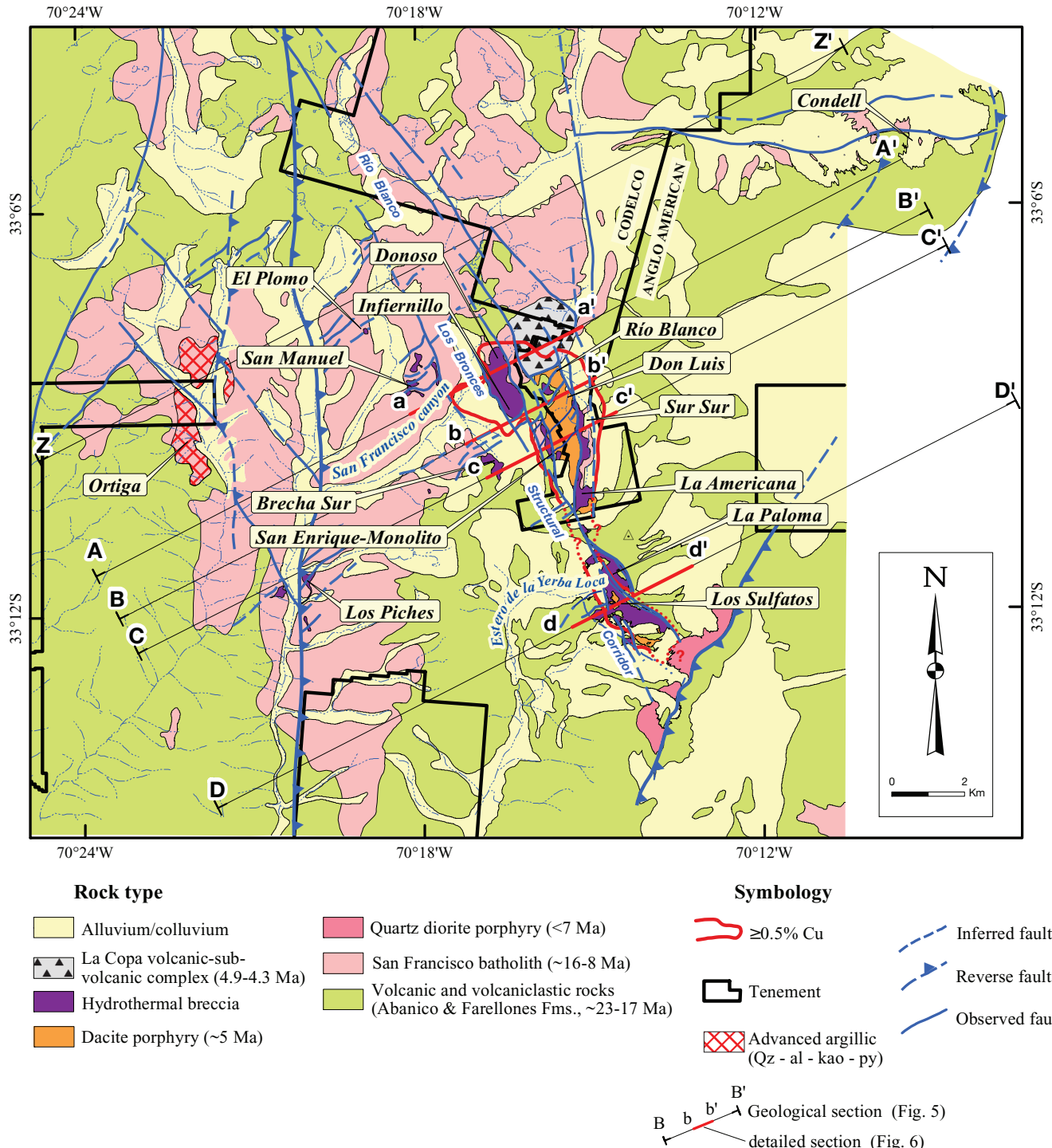


FIG. 3. Simplified geologic map of the Río Blanco-Los Bronces porphyry district, showing the locations of principal deposits and projects. Modified from Irarrazaval et al. (2010). Mineral abbreviations: al = alunite, kao = kaolinite, py = pyrite, qz = quartz.

and sigmoidal, centimeter-scale anhydrite-bearing fractures provide evidence for the syntectonic character of the magmatic and hydrothermal activity. Between 20 and 30% of the copper is associated with igneous- and hydrothermal-cemented breccias. Breccia infill includes rock flour, tourmaline, biotite, chlorite, specularite, and magnetite. The breccia

cement grades vertically from quartz-tourmaline-specularite-sericite-kaolinite-pyrite-chalcopyrite at shallow levels to quartz-biotite-K-feldspar-magnetite-chalcopyrite-bornite at deeper levels (Vargas et al., 1999). Hydrothermal assemblages bear consistent spatial relationships to multiphase diorite, quartz-monzonite, and dacite porphyry dikes. Crosscutting relationships

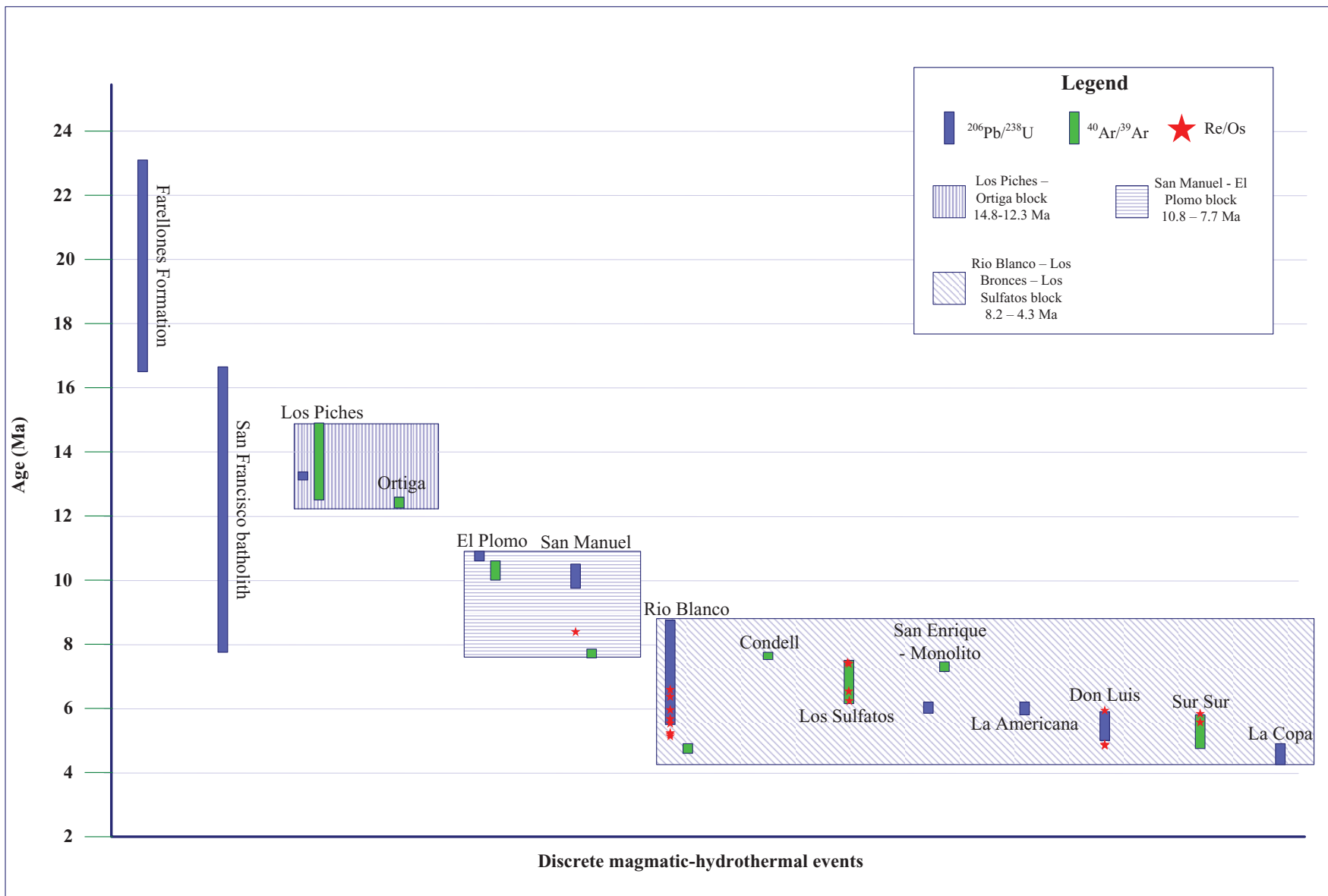


FIG. 4. Magmatic-hydrothermal history of the Rio Blanco-Los Bronces district.

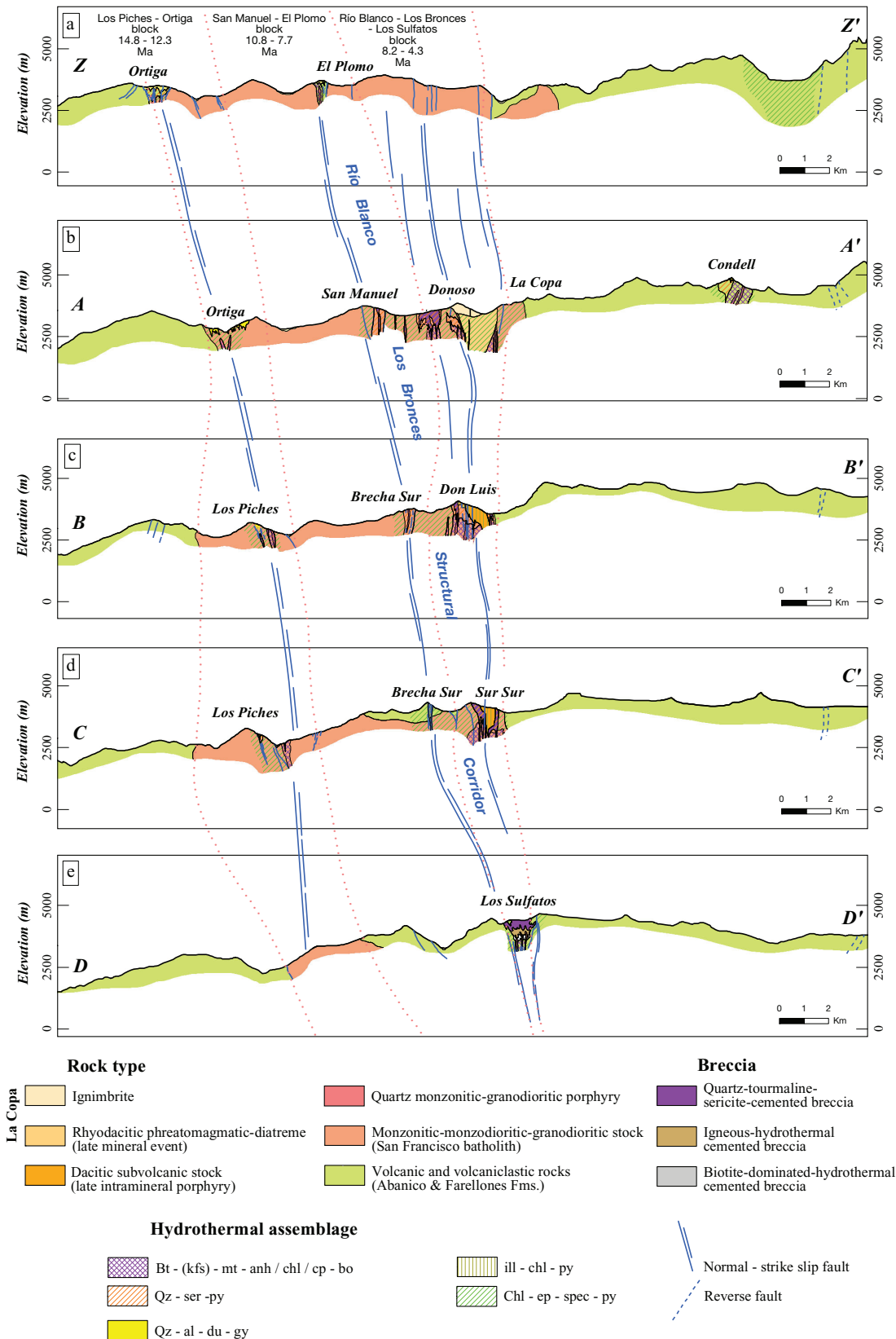


FIG. 5. Regional geologic sections, showing principal structural corridors controlling the distribution of magmatic-hydrothermal events in the Río Blanco-Los Bronces district. Mineral abbreviations: al = alumite, anh = anhydrite, bo = bornite, bt = biotite, chl = chlorite, cp = chalcopyrite, du = dumortierite, ep = epidote, kfs = K-feldspar, gy = gypsum, ill = illite, mt = magnetite, py = pyrite, qz = quartz, ser = sericite, spec = specularite.

TABLE 4. Summary of Breccia Facies Present at Río Blanco-Los Bronces District

Breccia type	Paragenetic position	Morphology/ dimensions (m)	Cementing minerals	Clast alteration assemblage	Clast rock types	Clast abundance (%)	Clast morphology	Crosscutting relationships	Associated Cu-Mo introduction	Occurrence
Late-magmatic	Premineral	Irregular/ 20 × 20–50	Magnetite, scapolite, tremolite, biotite, apatite, K-feldspar, epidote	Albite, K-feldspar, chlorite, tremolite	Quartz monzonite, andesite	5–30	Angular, irregular	Cut by EB-, A-, B-, C- and D-type veinlets	Low-barren	Bottom and margins of early intrusions; common in Los Piches and El Plomo
Igneous-hydrothermal	Early mineral	Irregular-diffuse/ 100–250 × 40–75	Igneous material (porphyries to aplite) and hydrothermal products and specularite, bornite, chalcopyrite	K-feldspar, albite	Andesite, quartz monzonite, porphyries and aplite	10–40	Irregular, angular	Some clasts contain truncated A-type veinlets	Main	Common in Los Sulfatos, Río Blanco, Don Luis, and San Enrique Monolito
Hydrothermal-biotite	Early intermineral	Diffuse/ 150–200 × 25–50	Biotite dominated, K-feldspar, chlorite, albite, quartz, anhydrite, bornite, chalcopyrite, pyrite	Biotite, chlorite, sericite	Andesite, quartz monzonite and porphyries	10–70	Subrounded, irregular	Cut by A-, B-, and C-type veinlets; lower parts are cut by EB-type veinlets	Main	Common in Los Sulfatos, Río Blanco, Sur-Sur, Monolito, and San Enrique
Hydrothermal-tourmaline	Intermineral	Upwardly flaring dikes/ 20–300 × 10–75	Quartz, tourmaline, sericite, pyrite, chalcopyrite	Sericite, kaolinite, illite, montmorillonite, chlorite	Andesite, granodiorite, quartz monzonite porphyry	30–70	Angular, irregular, subrounded	Cut by C- and D-type veinlets; lower parts are cut by A- and B-type veinlets	Main	Common in all the districts, mainly in Los Bronces complex breccias, Sur Sur, and Los Sulfatos
Rock-flour	Late mineral	Upwardly flaring dikes/ 10–750 × 2–500	Kaolinite, sericite, montmorillonite, pyrite	Kaolinite, sericite	Polymict, angular to subangular clasts	20–50	Subrounded, angular	Occasionally cut by tourmaline-cemented breccia dikes, and D- and DL-type veinlets; local quartz, pyrite, tennantite, chalcopyrite, galena, sphalerite, carbonate, gypsum veins	Low	The best example is the La Copá complex and several rock-flour-matrix breccias in Río Blanco, Los Sulfatos, and Don Luis

DL = D late, EB = early biotite, EBT = early biotite transitional

TABLE 5. Characteristics of Principal Veinlets Present in the Río Blanco-Los Bronces District

Veinlet type ¹ (alternative name)	Silicate assemblage	Alteration halo	Structural style	Sulfide assemblage	Position in the system	Economic relevance
EB (early biotite)	Biotite with varying proportions of albite, K-feldspar and actinolite	Albite	Discontinuous and sinuous	Chalcopyrite, bornite and minor pyrite	Deep	Ore contributor
EBT (early biotite transitional)	K-feldspar and coarse quartz	Biotite	Continuous and sinuous	Chalcopyrite, bornite and minor pyrite	Deep	Ore contributor
A	Quartz	K-feldspar	Continuous and sinuous	Chalcopyrite, bornite and local pyrite	Core zones	Main ore contributor
B	Quartz	Local K-feldspar	Regular and continuous	Chalcopyrite - Molybdenite and local pyrite	Core zones	Ore contributor
C	Quartz-green sericite and local biotite	Green sericite and local biotite	Regular and continuous	Chalcopyrite - bornite	Core zones	Ore contributor
D	Quartz and local tourmaline	Sericite	Regular and continuous	Pyrite and local chalcopyrite	Upper part	Locally constitutes ore
DL (D late)	Quartz and local tourmaline	Sericite-kaolinite	Regular and continuous	Massive pyrite	Upper part	Barren

¹ Veinlet nomenclature follows Gustafson and Hunt (1975; A, B, and D types) and Gustafson and Quiroga (1995; EB and C types)

suggest that collapse of the hydrothermal system coincided with emplacement of several subvolcanic bodies and development of a diatreme vent. Dacitic and andesitic dikes and local quartz-tourmaline-pyrite-chalcopyrite-cemented breccias emplaced within the diatreme represent the youngest recognized magmatic-hydrothermal activity in the block. Late-stage events, generally associated with NE-striking extensional faulting, comprise veins of quartz-pyrite-tennantite-enargite, galena, sphalerite, pyrite-chalcopyrite, gypsum-anhydrite, ankerite, and dolomite, with sericite, illite, kaolinite, or chlorite-epidote halos.

Río Blanco-Los Bronces and Los Sulfatos Deposit Geology

The geology of the Río Blanco-Los Bronces and Los Sulfatos deposits is discussed here in the context of four regional geologic cross sections (Fig. 3), which, from north to south, are: A-A': Los Bronces (Donoso)-Río Blanco; B-B': Brecha Sur-Don Luis complex; C-C': San Enrique-Monolito-Sur-Sur; and D-D': Los Sulfatos. Detailed geologic cross sections (Fig. 6) corresponding to the regional sections highlight the rock types and hydrothermal products in each mineralized center.

A summary of the breccia facies in the district is presented in Table 4, based on the nomenclature of Sillitoe (1985). Table 5 shows the district veinlet characteristics following the nomenclature of Gustafson and Hunt (1975) and Gustafson and Quiroga (1995) for the El Salvador porphyry deposit.

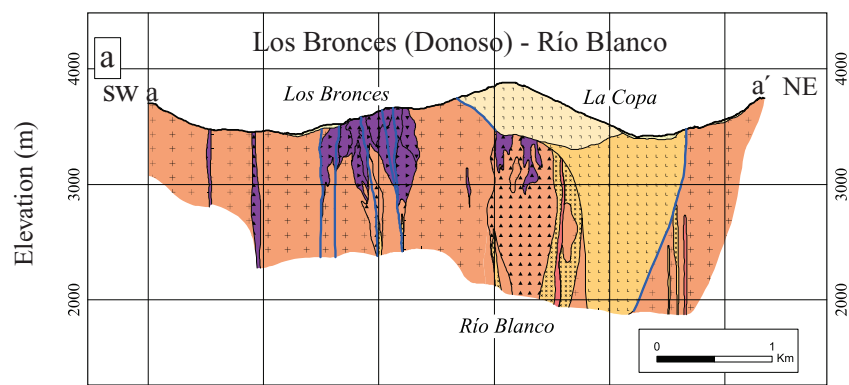
Section A-A' and a-a': Los Bronces (Donoso)-Río Blanco

Andesitic volcanic rocks of the Farellones Formation, characterized by porphyritic to aphanitic textures, underlie the Los Bronces sector. Intruding these rocks are several phases of the San Francisco batholith, comprising syenogranites, granodiorites, and quartz-monzonites displaying phaneritic equigranular and coarse holocrystalline textures. Three sub-sectors (described below) are distinguished in the area: Los

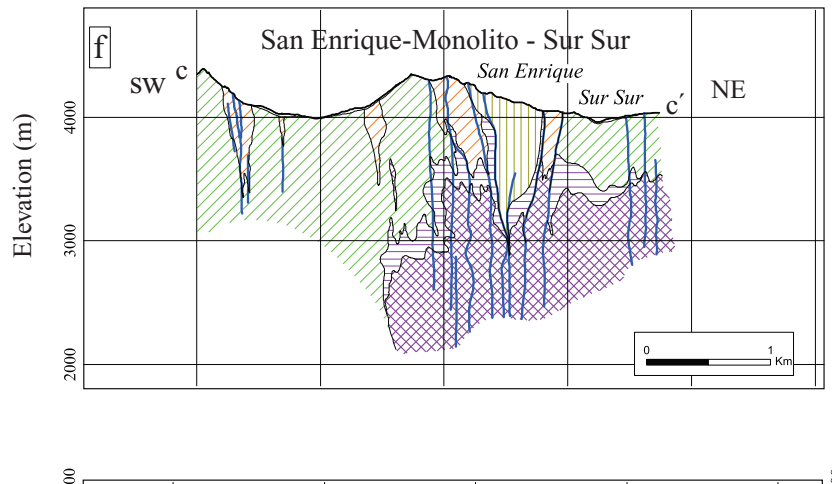
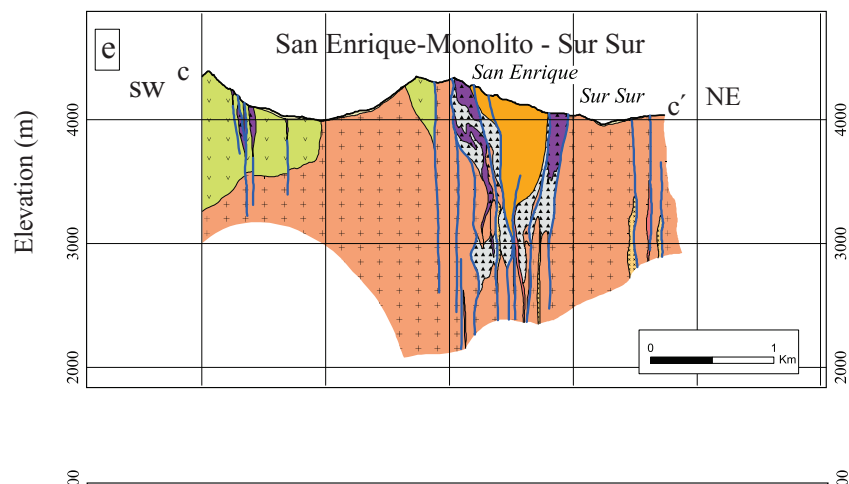
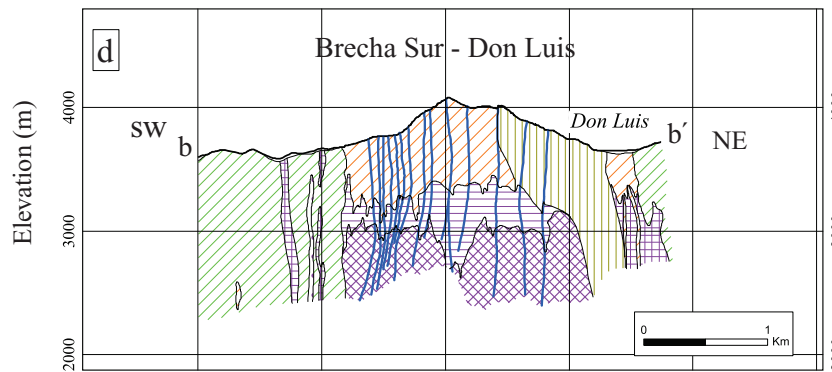
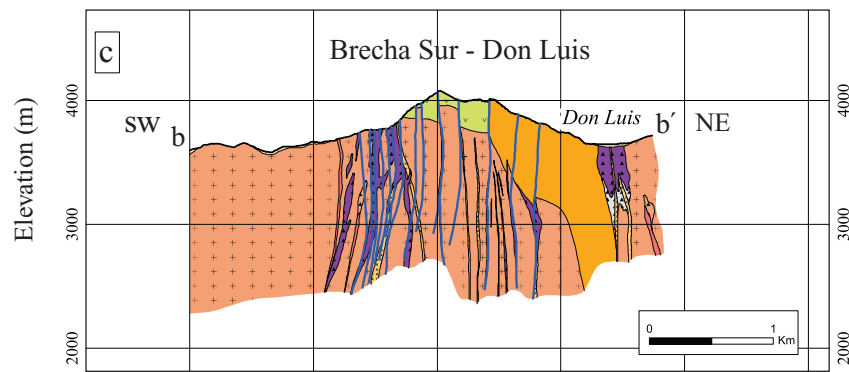
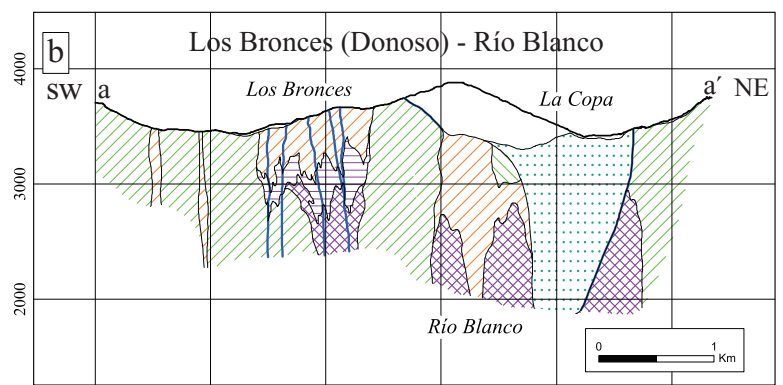
Bronces breccia complex, Río Blanco porphyry deposit, and La Copa complex (Figs. 3, 5a, 6a).

Los Bronces breccia complex: The Los Bronces breccia complex has been described in detail by Warnaars et al. (1985), Skewes and Holmgren (1993), Serrano et al. (1996), Vargas et al. (1999), and Skewes et al. (2003), and a brief summary is provided below. The complex covers an area of ~2 × 0.7 km, has a N-NW-S-SE orientation, and crops out between 4,150- and 3,450-m elevation (Figs. 3, 6a). There are at least seven coalesced breccia bodies, which are known (from older to younger) as the Fantasma, Central, Oeste, Infierillo, Anhidrita, Gris Fina, and Donoso breccias (Warnaars et al., 1985; Table 4). The breccias are distinguished on the basis of cement/matrix-contact relationships, clast types, alteration phases, and sulfide assemblages. There are three clast types recognized: andesite, quartz monzonite, and diorite; and several infill phases: quartz, tourmaline, specularite, anhydrite, pyrite, chalcopyrite, bornite, molybdenite, sericite, chlorite, and rock flour. Contact relationships are typically gradational. Hypogene copper contents increase progressively from the earliest to the latest breccia phase in the Los Bronces breccia complex. An assemblage of quartz-tourmaline-pyrite-chalcopyrite makes up the cement of the earliest breccia phases (Fantasma, Central and Oeste) with hypogene grades of up to 0.2% copper. Higher chalcopyrite contents differentiate the intermediate breccia phases (Infierillo, Anhidrita and Gris Fina) with hypogene grades of up to 0.6% copper. The highest hypogene copper grades correspond to the Donoso breccia, which is cemented by an assemblage of quartz-tourmaline, pyrite-chalcopyrite and chalcopyrite-bornite with average grades of 1% copper. In the Donoso breccia, high-grade bodies of chalcopyrite, pyrite, and specularite are distributed in irregular shells, in which one of the three minerals predominates in any one shell. Warnaars et al. (1985) described this texture as an onion-ring pattern, and these authors highlighted the rapid transitions between the shells. Within the Donoso breccia,

Rock type



Hydrothermal assemblage / zonation



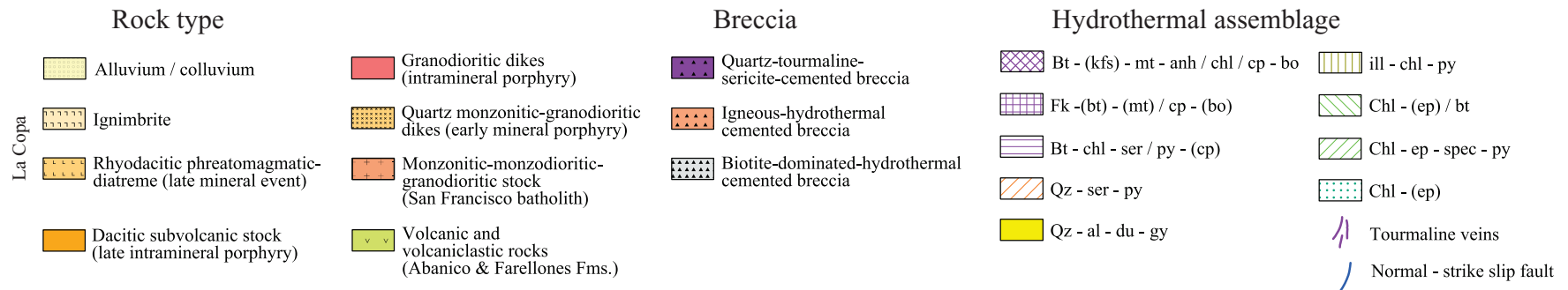
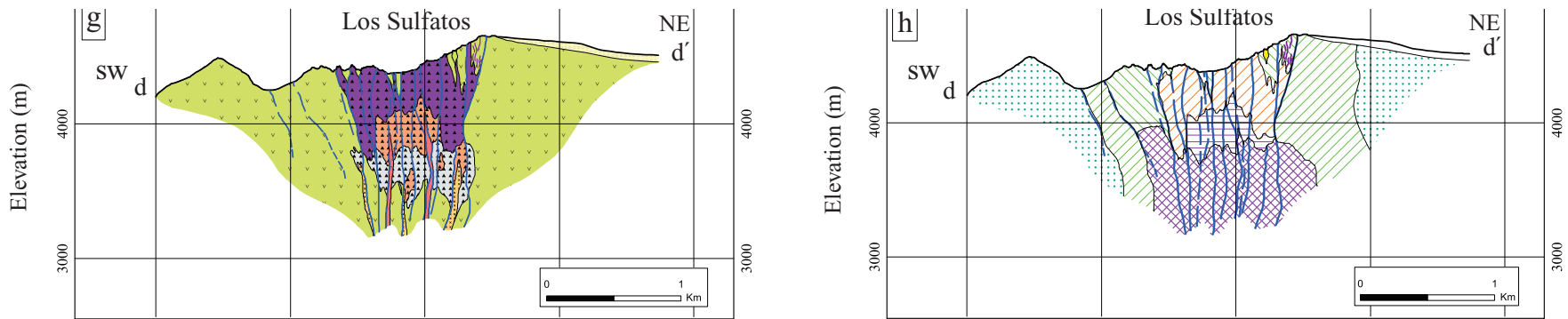


FIG. 6. Transverse southwest-northeast profiles through the Río Blanco-Los Bronces-Los Sulfatos deposits highlighting the north-south variations in hydrothermal assemblages and rock type controls. a. Los Bronces (Donoso)-Río Blanco rock type. b. Los Bronces (Donoso)-Río Blanco hydrothermal assemblage. c. Brecha Sur-Don Luis rock type. d. Brecha Sur-Don Luis hydrothermal assemblage. e. San Enrique-Monolito-Sur rock type. f. San Enrique-Monolito-Sur hydrothermal assemblage. g. Los Sulfatos rock type. h. Los Sulfatos hydrothermal assemblage. Mineral abbreviations: al = alumite, anh = anhydrite, bo = bornite, bt = biotite, chl = chlorite, cp = chalcopyrite, du = dumortierite, ep = epidote, kfs = K-feldspar, gy = gypsum, ill = illite, mt = magnetite, py = pyrite, qz = quartz, ser = sericite, spec = specularite.

high-grade bodies with direct-shipping ore containing 10 to 20% copper were the focus of mining activities at Los Bronces since its discovery in 1864. By 1920 the copper grade of the high-grade bodies dropped to 4.5% (Warnaars et al., 1985).

Río Blanco: The Río Blanco porphyry deposit, a N 30° W-striking intrusive and breccia complex, crops out 2 km east of Los Bronces over an area measuring 1,500 m in length, and between 250 and 800 m in width. This mineralized complex has a known vertical extent exceeding 1.4 km (Figs. 3, 6a). The oldest rocks in the area are andesitic and minor dacitic extrusive facies assigned to the Farellones Formation (J. Piquer and E. Wettke, unpub. report for CODELCO, 2010). Medium- to coarse-grained, granodioritic to tonalitic phases of the San Francisco batholith, locally named Río Blanco granodiorite, intrude the volcanic sequence. At shallow depths, a set of quartz-monzonite dikes follows the same N-NW orientation. The dikes have porphyritic textures and abundant plagioclase phenocrysts as well as quartz eyes and coarse biotite books set in a microfelsitic quartz-feldspar groundmass. Metal endowment at Río Blanco reflects the superposition of at least three main episodes of copper-molybdenum introduction (Fig. 6b): (1) biotitization of mafic minerals with early biotite and/or early biotite-sericite veinlets with chalcopyrite > bornite >> molybdenite and chlorite-epidote-pyrite halos (early biotite-type veinlets, Table 5); (2) specularite-cemented breccias with chalcopyrite >> bornite as disseminated grains and clots; (3) K-silicate alteration related to the quartz-monzonite porphyry, comprising A- and B-type veinlets and replacement of the rock-flour breccia matrix by K-silicate minerals (E. Tidy, unpub. report for CODELCO, 2009). This K-silicate assemblage is transitional, both laterally and vertically, to gray-green sericite. Four breccia types are distinguished at Río Blanco: igneous-cemented breccias, igneous/hydrothermal-cemented breccias, hydrothermal-cemented breccia, and rock-flour-matrix breccia (Table 4). These breccias make up a large proportion of the copper-molybdenum orebodies at Río Blanco (Serrano et al., 1996; Vargas et al., 1999). Hydrothermal-cemented breccias and rock-flour-matrix breccias represent the volumetrically most significant breccia bodies in this sector and are described in detail. The tourmaline-cemented breccia occupies the center of the mineralized body at Río Blanco. This breccia has a surface area of 300 × 150 m and extends over a vertical interval of 500 m. The breccia displays a transition from andesite clasts in the upper part to granodiorite clasts at depth. Up to 25% of the infill is tourmaline, with minor concentrations of biotite, quartz, anhydrite, sulfide minerals and, locally, rock flour. The rock-flour-matrix breccia forms a network of subvertical locally tabular bodies, ranging from centimeters to tens of meters in thickness, and is present over a vertical interval of 700 m. The rock-flour-matrix breccia contains polymictic, angular to subangular clasts. The light gray cement is composed of 25 to 50% hydrothermal biotite and/or K-feldspar at lower levels (2,500 m a.s.l.). The biotitization does not affect the central parts of large fragments. Sericite overprints biotite at shallow levels (>3,200 m a.s.l.; Fig. 6b). Locally, pervasive gray-green sericite affects the large fragments.

La Copa volcanic-subvolcanic complex: At the northwest extremity of Río Blanco, a complex comprising tuff/igneous-imbricate and several dacitic and rhyolitic dikes make up the La

Copa diatreme (Table 4; Figs. 5b, 6a). The dacitic part of the vent displays porphyritic, pyroclastic, and fragmental textures. It displays an upward-flaring morphology with steep wall angles, an average thickness of 200 m (at the current surface), and a vertical extent exceeding 1 km. Intense sericitic-illite alteration, with kaolinite having selectively replaced plagioclase phenocrysts, affects the dacitic vent. The rhyolitic vent, also with upward-flaring morphology, has a vertical extent exceeding 1 km. The rhyolite includes autoclastic fragmental phases and, locally, a boundary breccia that contains wall-rock fragments. At least 14 facies have been identified within the rhyolitic vent (Toro, 1986). The evidence for copper introduction during emplacement at La Copa is equivocal. At surface, NW-striking, narrow (0.3–1 m) dacitic dikes up to 60 m in length contain copper oxides (chrysocolla and malachite). CODELCO's drilling in 2007 intersected fragmental vent facies that were altered to tourmaline at depth and contained chalcopyrite. However, the paragenetic relationships between the dikes at surface, the mineralization intercepted at depth, and the La Copa complex is uncertain.

Alteration-mineralization of the Los Bronces (Donoso)-Río Blanco section: In the different breccia bodies of the Los Bronces (Donoso)-Río Blanco section, the hydrothermal cement is vertically zoned, from quartz, tourmaline, specularite, pyrite, and chalcopyrite cement (shallow levels) through igneous/hydrothermal-cemented breccias with quartz-tourmaline, anhydrite, chalcopyrite, pyrite, and local bornite cement (intermediate levels), to biotite-cemented breccias with chalcopyrite, bornite, and pyrite (at depth; Table 4; Fig. 6b). At shallow levels, and on the periphery of the breccia complex, a weakly developed concentric alteration zonation comprising a chlorite-kaolinite assemblage in the clast centers to a sericitic assemblage toward the clast margins affects the breccias. The roots of the breccia bodies grade transitionally into quartz-monzonite and diorite porphyry dikes that display abundant hydrothermal biotite, K-feldspar, anhydrite, magnetite, chalcopyrite, and bornite (Figs. 6a, b). The sulfide minerals are disseminated and also occur in A-, B-, C-, and D-type veinlets (Table 5). Specularite-anhydrite-cemented breccias, 30- to 50-m diameter, crosscut some of the above-mentioned units. These breccias display sericite-chlorite-clay assemblages with clots of chalcopyrite-bornite-chalcocite and enargite. Carbonate, tennantite/tetrahedrite and, locally, sphalerite and galena veins cut the specularite-anhydrite-cemented breccias.

Although the oldest U-Pb age at Río Blanco (obtained on the host Río Blanco granodiorite) is 12.0 ± 0.4 Ma (Table 3; Fig. 4), the earliest recognized hydrothermal events are considerably younger. Re-Os molybdenite ages determined for earliest recognized hydrothermal event range from 6.7 ± 0.03 to 6.48 ± 0.03 Ma. These overlap with U-Pb ages determined for the earliest porphyry phases in the area: 7.1 ± 0.2 to 6.48 ± 0.05 Ma (Table 3, Fig. 4). Re-Os molybdenite ages between 6.07 ± 0.03 and 5.65 ± 0.03 Ma were obtained for B-type veinlets from the latest recognized mineralized event at Río Blanco (Table 3, Fig. 4). These overlap with U-Pb ages determined for the feldspar porphyry: 5.92 ± 0.03 to 5.7 ± 0.1 Ma. The specularite-anhydrite-cemented breccias that crosscut the earlier breccia bodies yielded a sericite $^{40}\text{Ar}/^{39}\text{Ar}$ age of 4.71 ± 0.08 Ma (Table 3). At the La Copa complex, U-Pb zircon ages range

from 4.92 ± 0.09 to 4.57 ± 0.08 Ma, which were obtained for the dacitic vent, and a U-Pb zircon age of 4.31 ± 0.05 Ma that was obtained for the rhyolitic vent (Table 3, Fig. 4).

Section B-B' and b-b': Brecha Sur-Don Luis complex

Several geologic units have been identified in the area. These include the Sur breccia, Don Luis complex, tourmaline-cemented breccia, rock-flour-matrix breccia, Don Luis porphyry, and late breccias (Figs. 3, 5c, 6c), and are described below.

Sur breccia: Clasts of rock from the San Francisco batholith, cemented by quartz, tourmaline, sericite, and pyrite, make up the Sur breccia. The breccia is located 2 km west of Don Luis porphyry and crops out over an area of 0.5×0.5 km (Fig. 3). Tourmaline clots, with quartz-albite and pyrite halos have replaced the breccia at approximately 400 m below the surface. These clots are interpreted as the breccia root facies (Fig. 6c).

Don Luis complex: The Don Luis complex comprises andesitic roof pendants of the Farellones Formation, enveloped by granodiorite (Río Blanco granodiorite), quartz-monzonite (Cascada granodiorite), and diorite dikes of the San Francisco batholith (Fig. 6c). The Cascada granodiorite has a phaneritic, hypidiomorphic texture, and contains plagioclase and mafic phenocrysts in a fine-grained groundmass composed of quartz and feldspar. In the southeast of the Don Luis stock, diorite dikes intermingle with the Cascada granodiorite as subvertical, tabular bodies ~60 m thick (Fig. 6c).

Tourmaline-cemented breccia: The tourmaline-cemented breccia, located in the central parts of the area, is 300 m wide, elongate to the northwest, and extends vertically for 600 m. The breccia contains clasts of granitoid, diorite, and minor dacite porphyry affected by K-feldspar-albite and (locally) biotite alteration (Fig. 7a). Tourmaline and minor quartz, biotite, magnetite, and anhydrite cement the clasts. On its eastern and upper limits, the brecciation intensity decreases and grades into tourmaline-cemented crackle breccia. Completely recrystallized rock flour marks the lower limit of the breccia (E. Tidy, unpub. report for CODELCO, 2009). The tourmaline-cemented breccia bodies have truncated the dacite porphyries and are bounded by late rock-flour-matrix breccias in the north and west (Fig. 6c). A- and B-type quartz veinlets cut both the cement/matrix and fragments, implying that the breccias are early and potentially linked to the potassic alteration event. Intense superposition of gray-green sericite and late sericitic alteration is widespread (Fig. 6d).

Rock-flour-matrix breccia: A network of subvertical bodies up to 60 m thick makes up the rock-flour breccia immediately beneath the tourmaline-cemented breccia at elevations up to 2,500 m a.s.l. Intense K-silicate assemblages overprint the breccia at depth (<3,188 m; E. Tidy, unpub. report for CODELCO, 2009). The rock-flour-matrix breccia contains clasts of granitoid, dacite porphyry, andesite, and tourmaline-cemented breccia (Table 4; Figs. 7b, c). A fine-grained, fragmented aggregate of plagioclase, quartz, K-feldspar, and subordinate biotite, with tourmaline, quartz, and/or K-feldspar (commonly recrystallized), anhydrite, and magnetite makes up the breccia infill (E. Tidy, unpub. report for CODELCO, 2009).

Dacite porphyries (Don Luis porphyry): A series of late intermineralization dacite porphyry stocks, informally called

Don Luis porphyry, intrudes the aforementioned breccia bodies, locally reducing copper-molybdenum grades by dilution (Figs. 7d, e). The main dacite porphyry body has a dome-like morphology, expanding upward to a width of ~500 m over a vertical extent of 1.5 km. These porphyries show a pseudo-fractal, porphyritic texture, broken phenocrysts with reaction boundaries, and have individual plagioclase grains showing abundant glass inclusions (E. Tidy, unpub. report for CODELCO, 2009; Fig. 7f). An aggregate of microcrystalline quartz, K-feldspar, and erratic biotite makes up the porphyry groundmass. Dike-like dacite porphyry bodies (<20 m wide) have porphyritic textures, microcrystalline quartz-feldspar groundmass, and phenocrysts of plagioclase and minor quartz, K-feldspar, and biotite.

Late breccias: The latest recognized breccia events at Río Blanco-Los Bronces correspond to a tourmaline-cemented and rock-flour-matrix breccia containing clasts of dacite porphyry, granitoid, minor tourmaline, and andesite. This breccia body displays an upward-flaring morphology, with a width of 300 m at surface. Minor ($2-20 \times 0.5-3$ m) rock-flour-matrix breccia with elevated molybdenite or specularite also occurs within the Don Luis porphyry (Table 4).

Alteration-mineralization of the Brecha Sur-Don Luis complex section: Selective biotitization of ferromagnesian minerals, local K-feldspar replacement of plagioclase, and introduction of early biotite-, A-, and B-type veinlets (Table 4, 5) affects parts of the wall rocks (e.g. San Francisco batholith), the biotite-cement breccias, and the porphyry intrusions. This K-silicate event is the earliest recognized hydrothermal manifestation in the Sur-Don Luis complex section. Early biotite transitional-type, Table 5) veinlets have locally developed intense K-silicate stockworks in the wall rocks. An assemblage of biotite-K-feldspar-sericite containing minor chalcopyrite-bornite affects the rock-flour-matrix breccias (Fig. 6d). These altered rocks show a lateral zonation from biotite-K-feldspar-gray-green sericite in the mineralized cores, to gray-white sericite, to quartz-sericite externally (Fig. 6d). Lateral sulfide zonation varies commensurately from chalcopyrite-bornite in the cores, to pyrite > chalcopyrite, to pyrite >> chalcopyrite externally. The significant increase, from 2 to 3 to 3 to 5% in total sulfide content toward the margins of the deposit correlates with the lateral zoning of the alteration assemblage. Here a chlorite-epidote-bearing assemblage containing pyrite and erratic chalcopyrite forms a broad halo to the aforementioned K-silicate assemblage (Fig. 6d). Within the rocks in the deep portion of the Don Luis porphyry, an assemblage of biotite-K-feldspar with scarce early biotite transitional-, A-, and B-type veinlets, with low total sulfide contents (chalcopyrite > bornite) and lower copper-molybdenum content is interpreted as the second alteration-mineralization event in the Sur-Don Luis complex section (Fig. 6d). Processes of hydrothermal alteration developed an assemblage of albite-tourmaline and albite-tourmaline-chlorite along the margins of the porphyry intrusions. An assemblage of quartz and sericite with pyrite and local chalcopyrite overprints the earlier hydrothermal assemblage (Fig. 6d), and tennantite/tetrahedrite veins crosscut all the other assemblages described.

Zircon age determinations by chemical abrasion thermal ion mass spectrometry (CA-TIMS) for the dike-like porphyry intrusions at Don Luis (between 5.47 ± 0.01 and 5.35 ± 0.04

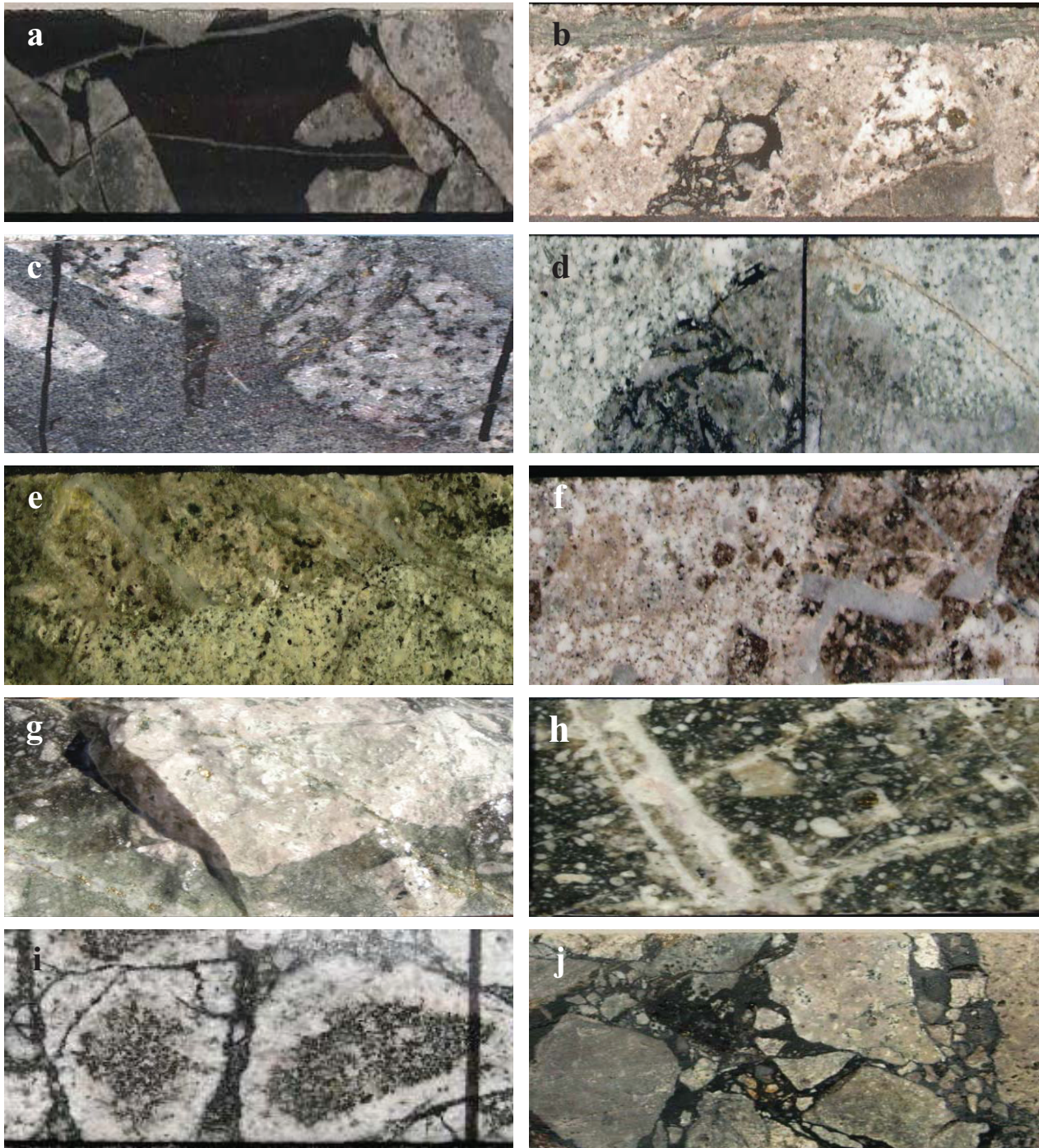


FIG. 7. a. Tourmaline-cemented breccia with subrounded clasts of dacitic porphyry/Don Luis. b. Rock-flour-matrix breccia with tourmaline-cemented breccia fragments, matrix partially recrystallized to quartz and K-feldspar. The B-type veinlets cut the matrix and fragments and D-type veinlets cut all the units. c. Rock-flour-matrix breccia with fragments of batholiths with truncated A-type veins as well as andesites fragments. d. Dacitic porphyry/Don Luis, with subangular clasts of tourmaline-cemented breccia with gray-green sericite. e. Dacitic porphyry cutting granodiorite sericite-chlorite with truncated A- and B-type veinlets. f. Porphyry breccia at the Don Luis porphyry, xenoliths of granodiorite are intensely altered to biotites. The xenoliths have truncated quartz veins, while quartz-molybdenite vein cut the matrix and fragments. g. Monolito breccias, showing volcanic and quartz- monzonitic clast cemented by an assemblage of chorite and magnetite. h. Monolito breccia, shows a fragmental texture with rock-flour-matrix cemented by biotite, anhydrite, K-feldspar, and tourmaline. Quartz veinlets developed K-feldspar and/or albite halos cutting the matrix/cement and fragments. i. Jigsaw-type texture tourmaline-cemented breccia. Granodiorites fragments are concentrically altered to secondary biotite on the center and to albite outside. The cement is made up of tourmaline and biotite. j. Polymictic tuffaceous tourmaline-cemented breccia with brown to black matrix composed of rock-flour and tourmaline. Fragments are affected by sericite and clay alteration.

Ma) are slightly younger than those obtained by isotope dilution thermal ion mass spectrometry (ID-TIMS; 5.84 ± 0.03 Ma; Table 3). Zircon age determinations by ID-TIMS and CA-TIMS obtained for the Don Luis porphyry (between 5.23 ± 0.07 and 5.0 ± 0.1 Ma) imply close temporal relationship with the emplacement of the dacitic vent (Table 3; Fig. 4). Molybdenite from a B-type veinlet of the earliest recognized hydrothermal event at Don Luis yielded an Re-Os age of 5.96 ± 0.03 Ma, and molybdenite from a B-type veinlet from the subsequent hydrothermal event yielded Re-Os ages between 4.90 ± 0.02 and 4.87 ± 0.02 Ma (Table 3; Fig. 4).

Section C-C' and c-c': San Enrique-Monolito-Sur-Sur

San Enrique-Monolito area: San Enrique-Monolito is an advanced exploration project located 2,000 m southeast of the Infiernillo-Los Bronces open pit and 1,100 m southeast of the Don Luis open pit (Fig. 3). This intrusive and breccia complex crops out over an area measuring more than 1.5 km north-south at an average elevation of 4,100 m a.s.l. A number of phases have intruded the stratified volcanosedimentary Farellones Formation. These include coarse-grained quartz monzonite, texturally and compositionally equivalent to the Río Blanco granodiorite (locally named the QM Gruesa), the Cascada granodiorite (QM Fina), a dacite porphyry (Observatorio porphyry), and a series of breccias (Monolito breccia, San Enrique breccia and tourmaline-rock-flour-matrix breccia; C. Sprohnle, W. Silva, and J. Zamorano, unpub. report for Anglo American Chile Ltda., 2007). Unconsolidated Quaternary deposits cover up to 60% of the area. The QM Gruesa quartz monzonite has a phaneritic, equigranular, and holocrystalline texture. As in the Brecha Sur-Don Luis complex (section B-B'), the Cascada granodiorite (QM Fina) intrudes the QM Gruesa. The QM Fina has a fine-grained, equigranular, locally porphyritic, and holocrystalline phaneritic texture. N-NW-oriented, dike-like diorite bodies have a locally porphyritic, seriate, and holocrystalline texture with vertical extensions of >1 km and widths of <30 m. Intruding the San Francisco batholith is the dacitic Observatorio porphyry, characterized by phenocrysts of plagioclase, K-feldspar, quartz, and minor biotite in a microcrystalline groundmass of quartz and K-feldspar. The Observatorio porphyry bodies have tabular forms, N to NE orientations, and thicknesses of up to 50 m. A moderate to weakly developed assemblage containing clots of chalcopyrite-magnetite and minor pyrite and weakly developed A- and B-type veinlets affects the Observatorio porphyry. D-type veinlets overprint all the hydrothermal events described above (R.H. Sillitoe, unpub. report for Anglo American Chile Ltda., 2008). A number of breccia bodies were formed after the emplacement of the Observatorio porphyry, the oldest recognized being the Monolito breccia. Located on the western side of the Sur Sur sector, the Monolito breccia has a horizontal extension of 840 m and recognized widths of up to 300 m (Fig. 6e). The Don Luis porphyry bounds the Monolito breccia to the north and east (Fig. 3). The Monolito breccia is polymictic, clast supported, and contains volcanic fragments near the surface and clasts of coarse-to fine-grained quartz-monzonite, tourmaline-cemented breccia and aplite at depth. An assemblage of chlorite-magnetite, grading to biotite-magnetite at depth cements the breccia (Fig. 7g). Within the Monolito breccia, which grades <0.5%

copper, chalcopyrite and pyrite are present as cement. A- and B-type veinlets cut the Monolito breccia infill, indicating its early mineralization character (Fig. 7h). The San Enrique breccia is polymictic, matrix supported, and has angular lithic fragments 2 to 6 mm in diameter (Table 4). Tourmaline, specularite, chalcopyrite, pyrite, and minor quartz and anhydrite/gypsum cement the breccia. A-, early biotite- and B-type and magnetite-chalcopyrite veinlets are confined to the clasts and evidently predate brecciation. D and D late (DL-type, Table 5) veins up to 30 cm in width cut the clasts and the cement of the breccia. The Don Luis porphyry intruded the aforementioned rocks in the northern area of San Enrique-Monolito. Small, dike-like (0.5–5 m wide) tourmaline-cemented rock-flour-matrix breccias developed along the western boundary of the Don Luis porphyry, near the San Enrique breccia. These breccias are matrix supported and have subrounded to rounded quartz-monzonite clasts containing hydrothermal sericite-tourmaline and disseminated pyrite > chalcopyrite. Hydrothermal associations at San Enrique-Monolito define three vertically arranged assemblages. A shallow (0–400 m) propylitic assemblage comprises chlorite-epidote-magnetite-pyrite cut by NE-trending quartz-sericite-kaolinite-pyrite veins/veinlets. This assemblage overprints and grades into an intermediate-depth (400–600 m) assemblage of chlorite-biotite-magnetite-chalcopyrite. An assemblage of biotite-chlorite-magnetite-chalcopyrite predominates at deep (>600 m) levels (Fig. 6f), where early biotite-, A-, B-, and early biotite transitional-type veinlets occur in the volcanic and intrusive rocks, and also cut the Monolito breccia (R. H. Sillitoe, unpub. report for Anglo American Chile Ltda., 2008).

Sur Sur area: The Sur Sur area is located 2 km east of San Enrique-Monolito and 1.5 km south of the Don Luis open pit (Fig. 3). The oldest rocks, porphyritic to aphanitic andesites, dip gently to the south and have thicknesses of ~200 m, thickening to the south. The Cascada granodiorite and diorite intrude these volcanic rocks. Porphyry dikes of dacitic composition, similar to the Observatorio porphyry in the La Americana sector (1.5 km south of Sur Sur, Fig. 3) intrude all the aforementioned units. Three mineralized units are distinguished in the area, the Sur Sur breccia complex, the Cascada granodiorite, and a diorite, described below. The Sur Sur breccia complex includes five types of breccia: tourmaline-cemented, biotite-cemented, Monolito, tuffaceous, and tuffaceous tourmaline-cemented breccia (Table 4). The main mineralized breccia, Sur Sur, is monomictic, clast supported, and tourmaline cemented with minor rotation of the wall-rock granitoids fragments, resulting in a jigsaw-type texture (Fig. 7i). The breccia has a subvertical, irregular, lens-like form extending 1 km north-south with a maximum width of 350 m (Stambuk et al., 1985; Serrano et al., 1996; R. Castagño, E. Book, and F. Fuentes, unpub. report for CODELCO, 2007). The breccia cement occupies an average of 15 vol % and comprises fine-grained tourmaline with minor quartz and magnetite-specularite. The hydrothermal assemblage of the breccia is vertically zoned from tourmaline-specularite in the upper parts, tourmaline > biotite at intermediate depths, and biotite-K-feldspar at the lowest levels (Vargas et al., 1999; Friksen, et al., 2005; R. Castagño, E. Book, and F. Fuentes, unpub. report for CODELCO, 2007). A-, B-, and C-type

veinlets, and (in the lower parts) early biotite transitional-type veins cut the breccia. The Monolito breccia (described above) truncates the Sur Sur breccia on its western side of the Don Luis porphyry and grades into quartz-monzonite on its eastern side. A polymictic, matrix-supported tourmaline-cemented breccia, with a high proportion of matrix (>50%), comprising (tuffaceous) rock flour and variable amounts of tourmaline as fragmental matrix, is the latest breccia phase recognized (Vargas et al., 1999). A hydrothermal assemblage of sericite and kaolinite intensely affects the clasts (Fig. 7j). Quartz-chalcopyrite-pyrite veinlets and quartz-K-feldspar-chalcopyrite veinlets with truncated gray-green sericite halos are common. The tuffaceous tourmaline-cemented breccia forms narrow, N-striking, dike-like bodies (<30 m wide) along the western side of the Sur Sur breccia above 3,638-m elevation; these bodies also cut the Monolito breccia. Replacement of plagioclase by K-feldspar, biotitized mafic minerals, partial sericitization of some plagioclase and sinuous biotite and/or quartz veinlets of fine-grained with K-feldspar halos affects the Cascada granodiorite and the diorite. Intense biotitization containing disseminated magnetite also affect the diorite. These assemblages are interpreted to represent deep-level K-silicate alteration events. Disseminated chalcopyrite-bornite-molybdenite and local early biotite-, early biotite transitional-, and/or A-type veinlets accompany the alteration.

Unpublished reports for CODELCO, by A. Bertens and E. Wettke (2008), reported a U-Pb zircon age of 17.2 ± 0.1 Ma for andesites assigned to the Farellones Formation on the Sur-Sur area (Table 3, Fig. 4). A U-Pb zircon age of 8.5 ± 0.1 Ma for a dioritic porphyry at San Enrique-Monolito area correlates well with the ages of the diorite at Don Luis (Table 3; Fig. 4). The intrusive affiliation of copper-molybdenum mineralization events at San Enrique-Monolito is unclear, although it may be relatively early, given a $^{40}\text{Ar}/^{39}\text{Ar}$ age determination for hydrothermal biotite of 7.2 ± 0.2 Ma (Table 3; Fig. 4). A U-Pb zircon age of 6.0 ± 0.1 Ma obtained from the Observatorio porphyry suggests a correlation with the fine-grained quartz-monzonite porphyries (Río Blanco and Don Luis), the dacite porphyry intrusions (located 2 km south of La Americana), and feldspar porphyries (Río Blanco and Don Luis), with U-Pb age determinations of 6.5 ± 0.1 , 6.0 ± 0.1 , and 5.84 ± 0.06 Ma, respectively (Table 3). Porphyry dikes of dacitic composition, similar to the Observatorio porphyry in the La Americana sector, yielded U-Pb zircon ages of 6.5 ± 0.1 and 6.0 ± 0.1 Ma (Table 3, Fig. 4). $^{40}\text{Ar}/^{39}\text{Ar}$ dating of sericite from the Sur-Sur breccia returned an age of 5.42 ± 0.09 Ma and Re-Os dating of molybdenite returned ages ranging from 5.79 ± 0.03 to 5.52 ± 0.03 Ma (Table 3; Fig. 4).

Section D-D' and d-d': Los Sulfatos

The Los Sulfatos area comprises a large, multiphase, igneous/hydrothermal-cemented breccia complex, with at least two separate centers of porphyry copper-style mineralization, one at Los Sulfatos and the other at La Paloma (Fig. 3). The mineralization occurs in a 6-km-long, N-NW-striking corridor to the south of the Sur Sur breccia. Subhorizontal to folded chlorite-epidote-pyrite-bearing volcanic and volcaniclastic rocks of the Abanico and Farellones Formations, affected by propylitic alteration (chlorite-epidote-pyrite) at surface, underlie the Los Sulfatos area (Fig. 6g, h). San Francisco

batholith intrudes these volcanic and volcaniclastic units. An assemblage of hydrothermal biotite ± K-feldspar with copper present in early biotite-, A-, and B-type veinlets (Table 5) strongly affects the southern side of Los Sulfatos stock and the volcanic rocks at depth.

Los Sulfatos stock: At least four discrete intrusive pulses formed a composite granodiorite porphyry stock at Los Sulfatos. Earliest recognized are two porphyry phases with crowded textures, abundant plagioclase, and minor mafic and quartz phenocrysts. A K-silicate assemblage (K-feldspar-biotite) containing chalcopyrite-bornite in A-type veinlets has affected these intrusions (Irarrázaval et al., 2010). Third in the intrusive sequence is a gray, intermineralization porphyry displaying fine-grained (chilled) margins against the crowded early porphyry intrusions. This intermineralization phase contains abundant A-type quartz veinlets with chalcopyrite. A late intermineralization granodiorite porphyry with a weak K-silicate assemblage, minor chalcopyrite, and lacking A-type veinlets is the final intrusive pulse recognized at Los Sulfatos (Irarrázaval et al., 2010). An assemblage of chlorite-sericite and later sericite-tourmaline overprints the high-grade center of the porphyry deposits, where the A-type veinlet intensity is greatest (Irarrázaval et al., 2010; Fig. 6h). In this zone, chalcopyrite-pyrite have replaced the original chalcopyrite-bornite assemblage and locally reduced grades to <0.4% copper (R. H. Sillitoe, unpub. report for Anglo American Chile Ltda., 2008).

La Paloma stock: Abundant quartz phenocrysts distinguish the La Paloma granodioritic porphyry center from the Los Sulfatos stock (Irarrázaval et al., 2010). The early porphyry phase contains abundant A-type and chalcopyrite-bornite veinlets, whereas two intermineralization facies are cut by only a few quartz veinlets and contain predominantly disseminated chalcopyrite ± bornite (Irarrázaval et al., 2010).

Igneous/hydrothermally-cemented breccias: Igneous/hydrothermal-cemented breccias are temporally related to the stocks at La Paloma and Los Sulfatos (Table 4). The breccia bodies contain andesite clasts with diffuse margins, as well as clasts of Los Sulfatos and La Paloma granodiorite porphyries. Some of the porphyry clasts contain truncated A-type veinlets. Igneous material, including porphyry, aplite, and a fine-grained rock, cements these breccias (Irarrázaval et al., 2010); the breccia cement may also include biotite, chalcopyrite, bornite, specularite, anhydrite, and late carbonate. Locally cutting the breccia are sulfide-rich veinlets, containing pyrite-chalcopyrite at shallow levels and chalcopyrite-bornite at depth (Irarrázaval et al., 2010). There are two main types of breccias with hydrothermal cement at Los Sulfatos, a shallow, tourmaline-cemented breccia and a deep, biotite-cemented breccia; contacts between the two are probably vertically transitional (Fig. 6g). The shallow, tourmaline-cemented breccia exposed between the La Paloma and Los Sulfatos area (Fig. 3) contains sericitized clasts of previously mineralized porphyry and andesitic country rocks (Table 4; Fig. 6h). A late assemblage of chalcopyrite, tennantite-tetrahedrite, galena, sphalerite, ankerite, and anhydrite in the cement makes up high-grade copper bodies (3–15% Cu), similar to the high-grade bodies described at Donoso by Warnaars et al. (1985). Chalcopyrite consistently occurs between the tourmaline and quartz and the ankerite cement. Near the surface, D-type

veinlets (pyrite-chalcopyrite) and rare chalcopyrite-molybdenite veinlets cut the tourmaline-cemented breccias. Minor volumes of rock-flour-matrix breccia occur at shallow levels in the La Paloma complex, where they are tentatively interpreted to predate the tourmaline-cemented breccia. Between 400 to 700 m below surface, the shallow, tourmaline-cemented breccia grades downward into biotite-cemented breccia (Table 4; Fig. 6g). Clast boundaries in the biotite-cemented breccia are unclear. The clasts are tightly packed and separated by minor cement comprising little more than hydrothermal biotite (Irarrázaval et al., 2010). Magnetite, chalcopyrite, bornite, and anhydrite are disseminated in both the clasts and cement. Although the tourmaline-cemented breccia locally cuts the biotite-cemented breccia, it is considered that the latter is the deep-level equivalent of the former, as noted previously at Sur-Sur (Frikken et al., 2005). The igneous/hydrothermally-cemented breccias tend to have chalcopyrite-bornite and less pyrite cement than the tourmaline-cemented breccia. At shallow levels and in the periphery a pyrite halo characterizes the Los Sulfatos system. Chlorite also occurs peripherally and locally overprints the K-silicate-dominated cores at La Paloma and Los Sulfatos (Fig. 6h). Remnants of advanced argillic alteration occurs as veins and ledges of chalcedony, dumortierite, alunite, pyrophyllite, native sulfur, and pyrite; outcrops are present at the highest elevations (>4,600 m; Fig. 6h) at Los Sulfatos.

Three $^{40}\text{Ar}/^{39}\text{Ar}$ age determinations on secondary biotite from Los Sulfatos yielded 7.3 ± 0.1 , 7.14 ± 0.08 , and 7.0 ± 0.1 Ma; two Re-Os age determinations on molybdenite gave 7.45 ± 0.05 and 7.42 ± 0.05 Ma; and two $^{40}\text{Ar}/^{39}\text{Ar}$ age determinations on sericite gave 6.94 ± 0.06 and 6.71 ± 0.04 Ma (Table 3, Fig. 4). At La Paloma, molybdenite samples returned Re-Os ages of 6.56 ± 0.05 and 6.26 ± 0.05 Ma (Table 3, Fig. 4).

Supergene Events

Vestiges of supergene-enriched rocks are preserved in the recently glaciated terrane of the Río Blanco-Los Bronces district. Supergene events affected the hydrothermal-cemented breccias at Infiernillo and San Enrique-Monolito. In Infiernillo the leached capping was not preserved, although partial secondary replacement of chalcopyrite-pyrite by chalcocite and minor covellite increase the copper grade from 0.4 to 0.6 to 0.9 to 1.2%. Patinas of supergene copper sulfides are observed at depths of up to 500 m. At San Enrique Monolito, the leached capping was not preserved and the supergene enrichment extends 200 m below the present surface. Here, high-grade supergene enrichment (>1% Cu) is only preserved beneath the Rinconada glacial moraine on the south side of San Enrique-Monolito (Fig. 3).

Discussion and Conclusions

Timing and duration of magmatic-hydrothermal activity

Geological and geochronological relationships presented here enable grouping of three porphyry-related magmatic-hydrothermal events (Table 3; Figs. 4, 5):

1. Intrusive and hydrothermal activity in the Los Piches-Ortiga block lasted ~2.5 m.y., from 14.8 ± 0.1 to 12.3 ± 0.1 Ma (Fig. 4). Although these events apparently did not produce

high-grade copper mineralization (recognized occurrences have grades of <0.3% Cu), silver-bearing veins associated with a high to intermediate sulfidation (enargite-tennantite-tetrahedrite/freibergite-bornite-chalcopyrite) assemblage are present in the block.

2. To the east in the San Manuel-El Plomo block, a series of magmatic-hydrothermal systems developed during a ~3 m.y. period between 10.8 ± 0.1 and 7.7 ± 0.1 Ma (Fig. 4). These events also apparently failed to generate more than low-grade copper mineralization. Porphyry emplacement at the Condell prospect (a poorly documented porphyry copper center approximately 5 km east of the El Plomo-San Manuel block) occurred toward the end of this period (7.61 ± 0.08 Ma).

3. Magmatic-hydrothermal activity in the eastern Río Blanco-Los Bronces-Los Sulfatos block, hosting virtually all of the copper endowment recognized in the district, spanned a ~4 m.y. period from 8.2 ± 0.5 to 4.31 ± 0.05 Ma (Fig. 4). The lifespan of magmatic-hydrothermal activity within a given block thus appears to have increased with progressive eastward migration of the underlying parental batholith and a concomitant migration of associated hydrothermal activity (Figs. 4, 5): 2.5 m.y. (Piches-Ortiga block), 3 m.y. (San Manuel-El Plomo block), and 4 m.y. (Río Blanco-Los Bronces-Los Sulfatos block).

The vast copper endowment of the Río Blanco-Los Bronces district is directly related to the magmatic-hydrothermal evolution of the San Francisco batholith. The oldest age determined in each block defines a progressive southwest to northeast emplacement of the San Francisco batholith between 16.4 ± 0.2 and 8.2 ± 0.5 Ma, a period of ~8 m.y. (Fig. 4). The timing of magmatic-hydrothermal activity related to the mineralizing events in the Río Blanco-Los Bronces district partly overlaps the middle and later stages of the emplacement of the San Francisco batholith (Fig. 4). The three magmatic-hydrothermal episodes, confined to three discrete structural blocks, document a complex history of magmatic-hydrothermal evolution that evolved over an interval of 10 to 11 m.y. While the protracted period of magmatic-hydrothermal activity for the Río Blanco-Los Bronces district as a whole exceeds that of all other districts in the Miocene-Pliocene copper-molybdenum porphyry belt of central Chile and Argentina, the ~4-m.y. period defined for porphyry development in the Río Blanco-Los Bronces-Los Sulfatos block is comparable in duration to those of other major porphyry districts in the belt. Earlier workers have defined a ~3-m.y. magmatic-hydrothermal history for the El Teniente deposit, located 100 km south (94 Mt Cu; Camus, 2003; Maksaev et al., 2004; Vry et al., 2010); a 3.8-m.y. period for the Los Pelambres deposit, located 150 km north (37 Mt Cu: Perello et al., 2012); and a 6-m.y. period for the San Felipe district, located 60 km to the north (Ortízar, 2006; Toro et al., 2006, 2009). This multistage magmatic-hydrothermal evolution is considered a key factor that contributed to the considerable volume of high-grade copper-molybdenum porphyry systems in the Río Blanco-Los Bronces district.

Structural focus of fluids and magmas

The emplacement of the multiple porphyry intrusions and breccia complexes in the district were controlled by the

N-NW-striking Río Blanco-Los Bronces-Los Sulfatos structural corridor (Figs. 3, 5). This structural trend varies from narrow (1 km) and focused in the south (Los Sulfatos) to broad (4 km) and diffuse in the north (El Plomo; Fig. 5). We speculate that the focus of multistage magmatic-hydrothermal activity within the relatively narrow southern end of this structural corridor likely played an important role in developing the large and high-grade copper systems in the district. Where the fault systems diverge and broaden, to the north, lower grade porphyry and breccia bodies developed (El Plomo). Still farther north, the structural corridor widens progressively, with fewer and lower grade copper systems.

Spatial distribution of hydrothermal assemblages

Hydrothermal assemblages follow a characteristic zonation pattern largely controlled by depth below the inferred paleosurface. Remnants of high to intermediate sulfidation assemblages and advanced argillic alteration (quartz-enargite-tennantite-galena-sphalerite-gypsum-anhydrite with dumortierite-pyrophyllite-alunite) and peripheral sericite-illite reflect preservation of shallow levels, whereas K-silicate alteration assemblages (biotite-K-feldspar-albite) have developed in association with chalcopyrite-bornite-pyrite at depth (Fig. 6). Between the mineralized bodies, a distal assemblage of hydrothermal chlorite-epidote-specularite-pyrite predominates. The mineralized bodies at Río Blanco-Los Bronces occur as aligned clusters characterized by igneous/hydrothermal- and hydrothermal-cemented breccias (Table 4) that developed in intimate association with porphyry phases. At shallow depths, the hydrothermal breccia cement generally comprises quartz-sericite-tourmaline and contains pyrite > chalcopyrite/molybdenite (Fig. 6). At deeper levels the breccia cement is predominantly biotite-K-feldspar (and locally magnetite) containing bornite-chalcopyrite-molybdenite. This deeper assemblage grades progressively outward into chalcopyrite-pyrite- and ultimately to pyrite-dominated zones (Fig. 6).

The vertical extent and spatial relationships between shallow and deep alteration assemblages in the Río Blanco-Los Bronces-Los Sulfatos block reveal varying degrees of “telescoping” (overprinting) of higher temperature (K-silicate) hydrothermal phases by lower temperature (feldspar-destructive) assemblages. A useful reference datum within the hydrothermal system is the elevation of the transition between deeper K-silicate (biotite-K-feldspar) and shallower post-K-silicate (feldspar-destructive) assemblages. Within the Río Blanco-Los Bronces-Los Sulfatos block, the “roof” of the K-silicate assemblage varies from ~3,000 m a.s.l. in the north (Río Blanco; Fig. 6b), to ~4,000 m a.s.l in the south (Los Sulfatos; Fig. 6h). At Río Blanco, the vertical extent of alteration and breccia facies exceeds 1,500 m, with minimal overprinting of K-silicate assemblages by feldspar-destructive alteration assemblages. In contrast, at Los Sulfatos the advanced-argillic and K-silicate assemblages are compressed over a narrower (<800 m) vertical range, with a considerably greater degree of telescoping. These differences may reflect varying rates of synmineral structural exhumation, or varying porphyry emplacement depths, along the Río Blanco-Los Bronces-Los Sulfatos structural corridor.

Tectonic context of giant porphyry formation

Several lines of inquiry including fluid inclusion studies (e.g., Skewes and Holmgren, 1993), geomorphologic analysis (Farias et al., 2008), and fission track dating (e.g., Maksaev et al., 2009) suggest that the central Chilean Andes (33° – 35° S) experienced a temporally discrete period of peak compression and rapid exhumation in the late Miocene-early Pliocene. Maksaev et al. (2009) documented an episode of enhanced crustal cooling for the central Chilean Andes between ~6 and 3 Ma, consistent with accelerated exhumation rates. This period overlaps part of the emplacement history of the Río Blanco-Los Bronces-Los Sulfatos block (8.2–4.31 Ma), and follows the last significant phase of volcanism documented for the district (Table 3).

Enhanced late Miocene surface uplift and erosion in the central Chilean Andes relates to the onset of slab shoaling due to subduction of seafloor containing the Juan Fernandez Ridge into the Chile Trench (Yáñez et al., 2002), a setting currently marked by the zone of modern volcanic quiescence between ~ 27° S and 33° S in central Chile (Fig. 1). Numerous authors (e.g., James and Sacks, 1999; Gutscher et al., 2000; Kerrich et al., 2000; Cooke et al., 2005; Hollings et al., 2005) have discussed the spatial and temporal relationship between flat-slab subduction settings and the formation of significant porphyry and related deposits. Under such conditions, enhanced horizontal crustal compression related to increased coupling from perturbations on the downgoing slab is thought to promote the retention of magma in the deep crustal environment, minimizing the loss of the volatile and metal load of the magma to the atmosphere during eruptive events (e.g., McClay et al., 2002; Skarmeta et al., 2003; Gow and Walshe, 2005). With higher attendant pressures, deep crustal magma retention also enhances the solubility of water and related volatiles within the magma. Similarly, higher ambient temperatures slow fractionation processes, increasing magma chamber longevity, and enhancing the potential for increasing the metal and volatile load by progressive addition of unfractuated magma batches (e.g., Cooke et al., 2005; Rohrlach and Loucks, 2005; Loucks, 2012).

Within the broader context of flat-slab subduction associated with the Juan Fernandez Ridge, it is proposed that the absence of documented volcanism coinciding with the most significant periods of copper introduction, and the protracted history of magmatism presented herein for the Río Blanco-Los Bronces district, are consistent with features of compressive arc settings that promote the conditions of magma fertility described above. Within the Río Blanco-Los Bronces-Los Sulfatos block in particular, the narrow structural focus of magmas and hydrothermal fluids, and the long-lived (~4 m.y.) period of porphyry formation are considered to be key factors contributing to the largest documented accumulation of copper on Earth.

Acknowledgments

We thank Anglo American, particularly Tracey Kerr (Group Head of Exploration) and Vicente Irarrázaval (Head of Exploration, Andes Region), and CODELCO, particularly Carlos Huete (Exploration Manager), for facilitating preparation of this paper. We also thank constructive reviews and comments

from Richard Sillitoe, Jeffrey Hedenquist, Lew Gustafson, Francisco Camus, and Victor Maksaev. Our colleague Dave Braxton is gratefully acknowledged for his thorough reviews and discussions, which improved the quality of the manuscript. Thanks are also due to Julio Bravo of Anglo American Chile for digitization of the figures.

REFERENCES

- Anglo American plc, 2009a, Anglo American announces new San Enrique Monolito copper prospect in Chile with Inferred Resources of 900 million tonnes: <http://www.angloamerican.co.uk/aa/media/releases/2009pr/2009-07-31/>.
- , 2009b, Anglo American announces new Los Sulfatos copper prospect in Chile with Inferred Resources of 1.2 billion tonnes: <http://www.angloamerican.co.uk/aa/media/releases/2009pr/2009-07-31a>.
- , 2012, Annual report 2011: London, Anglo American plc, 226 p.
- Baeza, R.S., 1990, Chile país minero: Historia del mineral de Las Condes: Santiago, Chile, Museo Histórico Nacional, 32 p.
- Cahill, T., and Isaacs, B., 1992, Seismicity and shape of the subducted Nazca plate: *Journal of Geophysical Research*, v. 97, p. 503–529.
- Camus, F., 2003, Geología de los sistemas porfíricos en los Andes de Chile: Santiago, Chile, Servicio Nacional de Geología y Minería, 267 p.
- Cannell, J., Cooke, D.R., Walshe, J.L., and Stein, H., 2005, Geology, mineralization, alteration, and structural evolution of the El Teniente porphyry Cu-Mo deposit: *Economic Geology*, v. 100, p. 979–1003.
- Cooke, D.R., Hollings, P., and Walshe, J.L., 2005, Giant porphyry deposits—characteristics, distribution and tectonic controls: *Economic Geology*, v. 100, p. 801–818.
- Correa, C., 1975, Historia sobre la legislación cuprífera en Chile, in Zauschkevich, A., and Sutulov, A., eds., *El Cobre Chileno*: Corporación del Cobre, p. 63–115.
- Deckart, K., Clark, A.H., Aguilar, C., Vargas, R., Bertens, A.N., Mortensen, J.K., and Fanning, M., 2005, Magmatic and hydrothermal chronology of the giant Río Blanco porphyry copper deposit, central Chile: Implications of an integrated U-Pb and $^{40}\text{Ar}/^{39}\text{Ar}$ database: *Economic Geology*, v. 100, p. 905–934.
- Deckart, K., Silva, W., Toro, J.C., and Bertens, A., 2009, New geochronology of the Los Bronces porphyry: Implication for mineral exploration on the Río Blanco-Los Bronces cluster: Congreso Geológico Chileno, 12th, Santiago, 2009, Actas, Pendrive, p. S11–012.
- Deckart, K., Clark, A.H., Cuadra, P., and Fanning, M., 2012, Refinement of the time-space evolution of the giant Mio-Pliocene Río Blanco-Los Bronces porphyry Cu-Mo cluster, Central Chile: New U-Pb (SHRIMP II) and Re-Os geochronology and $^{40}\text{Ar}/^{39}\text{Ar}$ thermochronology data: *Mineralium Deposita*, DOI 10.1007/s00126-012-0412-9.
- Eggers, T., 2009, Alteración argilicá avanzada en el distrito Los Bronces: Congreso Geológico Chileno, 12th, Santiago, 2009, Actas, Pendrive, p. S11–013.
- Farías, M., Charrier, R., Carretier, S., Martinod, J., Fock, A., Campbell, D., Cáceres, J., and Comte, D., 2008, Late Miocene high and rapid surface uplift and its erosional response in the Andes of central Chile (33° – 35° S): *Tectonics* 27, TC 1005, doi:10.1029/2006TC002046.
- Frikken, P.H., Cooke, D.R., Walshe, J.L., Archibald, D., Skarmeta, J., Serrano, L., and Vargas, R., 2005, Mineralogical and isotopic zonation in the Sur-Sur tourmaline breccia, Río Blanco-Los Bronces Cu-Mo deposit, Chile: Implications for ore genesis: *Economic Geology*, v. 100, p. 935–962.
- Gow, P., and Walshe, J.L., 2005, The role of preexisting geologic architecture in the formation of giant porphyry-related Cu ± Au deposits: Examples from New Guinea and Chile: *Economic Geology*, v. 100, p. 819–833.
- Gustafson, L.B., and Hunt, J.P., 1975, The porphyry copper deposit at El Salvador, Chile: *Economic Geology*, v. 70, p. 856–912.
- Gustafson, L.B., and Quiroga G., J., 1995, Patterns of mineralization and alteration below the porphyry copper orebody at El Salvador, Chile: *Economic Geology*, v. 90, p. 2–16.
- Gutscher, M.A., Spakman, W., Bijwaard, H., and Engdahl, E.R., 2000, Geodynamics of flat slab subduction: Seismicity and tomographic constraints from the Andean margin: *Tectonics* v. 19, p. 814–833.
- Hollings, P., Cooke, D., and Clark, A., 2005, Regional geochemistry of Tertiary igneous rocks in central Chile: Implications for the geodynamic environment of giant porphyry copper and epithermal gold mineralization: *Economic Geology*, v. 100, p. 887–904.
- Irarrázaval, V., Sillitoe, R.H., Wilson, A., Toro, J.C., Robles, W., and Lyall, G., 2010, Discovery history of a giant, high-grade, hypogene porphyry copper-molybdenum deposit at Los Sulfatos, Los Bronces-Río Blanco district, central Chile: Society of Economic Geologists Special Publication 15, p. 253–270.
- James, D.E., and Sacks, I.S., 1999, Cenozoic formation of the Central Andes: A geophysical perspective: Society of Economic Geology Special Publication 7, p. 1–26.
- Kay, S.M., and Mpodozis, C., 2002, Magmatism as a probe to the Neogene shallowing of the Nazca plate beneath the modern Chilean flat-slab: *Journal of South American Earth Sciences*, v. 15, p. 39–57.
- Kerrick, R., Goldfarb, R., Groves, D., and Garvin, S., 2000, The geodynamics of world-class gold deposits: Characteristics, spacetime distributions, and origins: *Reviews in Economic Geology*, v. 13, p. 501–551.
- Kurtz, A., Kay, S.M., Charrier, R., and Farrar, E., 1997, Geochronology of Miocene plutons and Andean uplift history in the El Teniente region, central Chile (34° – 35° S): *Revista Geológica de Chile*, v. 24, p. 75–90.
- Loucks, R.R., 2012, Chemical characteristics, geodynamic settings, and petrogenesis of copper-ore-forming arc magmas: Centre for Exploration Targeting, University of Western Australia, Quarterly News 19, p. 1–10.
- Maksaev, V., Munizaga, F., McWilliams, M., Fanning, M., Mathur, R., Ruiz, J., and Zentilli, M., 2004, New chronology for El Teniente, Chilean Andes, from U-Pb, $^{40}\text{Ar}/^{39}\text{Ar}$, Re-Os, and fission track dating: Implications for the evolution of a supergiant porphyry Cu-Mo deposit: Society of Economic Geologists Special Publication 11, p. 15–54.
- Maksaev, V., Munizaga, F., Zentilli, M., and Charrier, R., 2009, Fission track thermochronology of Neogene plutons in the Principal Andean Cordillera of central Chile (33° – 35° S): Implications for tectonic evolution and porphyry Cu-Mo mineralization: *Andean Geology*, v. 36, p. 153–171.
- Mathur, R., Ruiz, J.R., and Munizaga, F.M., 2001, Insights into Andean met-allogenesis from the perspective of Re-Os analysis of sulfides [ext. abs.]: South American Symposium on Isotope Geology, 3rd, Pucón, Chile, 2001, Extended Abstracts, CD-ROM, p. 500–503.
- McClay, K., Skarmeta, J., and Bertens, A., 2002, Structural controls on porphyry copper deposits in northern Chile: New models and implications for Cu-Mo mineralization in subduction orogens: *Australian Institute of Geoscientists Bulletin*, v. 36, p. 127.
- Olivarría, A., 2009, Planes de Andina agregan más cobre fino a Codeleco: Nueva Minería y Energía [Chile], yr. 1, no. 6, p. 52–59.
- Ortúzar, J., 2006, Geología del Prospecto Novicio, Alta Cordillera, 5^a Región, Chile Central: Memoria de Titulo (Inédito), Universidad de Chile, 87 p.
- Perelló, J., Sillitoe, R.H., Brockway, H., Posso, H., and Mpodozis, C., 2009, Contiguous porphyry Cu-Mo and Cu-Au mineralization at Los Pelambres, central Chile: Congreso Geológico Chileno, 12th, Santiago, 2009, Actas, Pendrive, 4 p.
- Perelló, J., Sillitoe, R.H., Mpodozis, C., Brockway, H., and Posso, H., 2012, Geologic setting and evolution of the porphyry copper-molybdenum and copper-gold deposits at Los Pelambres, central Chile: *Economic Geology*, v. 108, p. 79–104.
- Ramos, V.A., Cristallini, E.O., and Pérez, D.J., 2002, The Pampean flat-slab of the Central Andes: *Journal of South American Earth Sciences*, v. 15, p. 59–78.
- Rohrlach, B.D., and Loucks, R.R., 2005, Multi-million-year cyclic ramp-up of volatiles in a lower crustal magma reservoir trapped below the Tampakan copper-gold deposit by Mio-Pliocene crustal compression in the Southern Philippines, in T.M. Porter, T.M., ed., Super porphyry copper and gold deposits—a global perspective: Australia, Porter GeoConsulting Publishing, v. 2, p. 369–407.
- Serrano, L., Vargas, R., Stambuk, V., Aguilar, C., Galeb, M., Holmgren, C., Contreras, A., Godoy, S., Vela, I., Skewes, M.A., and Stern, C.R., 1996, The late Miocene to early Pliocene Río Blanco-Los Bronces copper deposit, central Chilean Andes: Society of Economic Geologists Special Publication 5, p. 119–130.
- Sillitoe, R., 1985, Ore-related breccias in volcanoplutonic arcs: *Economic Geology*, v. 80, p. 1467–1514.
- Sillitoe, R.H., and Perelló, J., 2005, Andean copper province: Tectonomagnetic settings, deposit types, metallogeny, exploration, and discovery: *Economic Geology* 100th Anniversary Volume, p. 845–890.
- Silva, W., Toro, J.C., and Bertens, A., 2009, Mineralización primaria sintética en el distrito minero Río Blanco-Los Bronces: Congreso Geológico Chileno, 12th, Santiago, 2009, Actas, Pendrive, p. S11–059.
- Skarmeta, J., McClay, K., and Bertens, A., 2003, Structural controls on porphyry copper deposits in northern Chile: New models and implications for

- Cu-Mo mineralisation in subduction orogens: Actas - 10º Congreso Geológico Chileno, Concepción, 2003.
- Skewes, M.A., and Holmgren, C., 1993, Solevantamiento andino, erosión y emplazamiento de brechas mineralizadas en el depósito de cobre porfídico Los Bronces, Chile central (33°S): Aplicación de geotermometría de inclusiones fluidas: Revista Geológica de Chile, v. 20, p. 71–83.
- Skewes, M.A., and Stern, C.R., 1995, Genesis of the giant late Miocene to Pliocene Cu deposits of Central Chile in the context of Andean magmatic and tectonic evolution: International Geology Reviews, v. 37, p. 893–909.
- Skewes, A.M., Arévalo, A., Floody, R., Zuñiga, P.H., and Stern, C.R., 2002, The giant El Teniente breccia deposit: Hypogene copper distribution and emplacement: Society of Economic Geologists Special Publication 9, p. 299–332.
- Skewes, M.A., Holmgren, C., and Stern, C.R., 2003, The Donoso copper-rich, tourmaline-bearing breccia pipe in central Chile: Petrologic, fluid inclusion and stable isotope evidence for an origin from magmatic fluids: Mineralium Deposita, v. 38, p. 2–21.
- Stambuk, V., Serrano, L., and Vargas, R., 1985, Geología del sector Sur-Sur, yacimiento Río Blanco: Congreso Geológico Chileno, 4th, Antofagasta, Actas Tomo 2, p. 383–404.
- Stern, C.R., 1989, Pliocene to Present migration of the volcanic front, Andean southern volcanic zone: Revista Geológica de Chile, v. 16, p. 145–162.
- Toro, J.C., 1986, Cuerpos subvolcánicos asociados a zonas de alteración hidrotermal en la alta cordillera de Chile Central: Antofagasta, Chile, Departamento de Geociencias, Universidad del Norte, Unpublished Memoria de Título, 174 p.
- Toro, J.C., Ortúzar, J., Maksnev, V., Barra, F., and Zamorano, J., 2006, Cronología de un nuevo cluster en la franja de porfidos cupríferos del mioceno de Chile central: Geocronología: Congreso Geológico de Chile, XI, Antofagasta.
- Toro, J.C., Ortúzar, J., Maksnev, and Barra, F., 2009, Nuevos antecedentes geocronológicos franja de pórfidos Cu-Mo del Mioceno-Plioceno, Chile central: Implicancias metalogénicas: Congreso Geológico Chileno, 12th, Santiago, 2009, Actas, Pendrive, 4 p.
- Vargas, R., Gustafson, L.B., Vukasovic, M., Tidy, E., and Skewes, M.A., 1999, Ore breccias in the Río Blanco-Los Bronces porphyry copper deposit, Chile: Society of Economic Geologists Special Publication 7, p. 281–297.
- Vry, V.H., Wilkinson, J.J., Seguel, J., and Millán, J., 2010, Multistage intrusion, brecciation, and veining at El Teniente, Chile: Evolution of a nested porphyry system: Economic Geology, v. 105, p. 119–153.
- Warnaars, F.W., Holmgren, C., and Barassi, S., 1985, Porphyry copper and tourmaline breccias at Los Bronces-Río Blanco, Chile: Economic Geology, v. 80, p. 1544–1565.
- Yáñez, G., Cembrano, J., Pardo, M., Ranero, C., and Sellés, D., 2002, The Challenger-Juan Fernández-Maipo major tectonic transition of the Nazca-Andean subduction system at 33°–34°S: Geodynamic evidence and implications: Journal of South American Earth Sciences, v. 15, p. 23–38.